LEBANESE AMERICAN UNIVERSITY

A Stackelberg Game Inspired Model of Real-Time Economic Dispatch with Demand Response

By

Youssef Shakrina

A thesis

Submitted in partial fulfillment of the requirements for the degree of Master of Science in Engineering

School of Engineering

May 2021

LAU
الجامعة اللبنانية الأميركية
Lebanese American University

THESIS APPROVAL FORM

Student Name: Youssef Shakrina I.D. #: 201501115

Thesis Title: A Stackelberg Game Inspired Model of Real-Time Economic Dispatch with Demand Respc

Program: MSE in Computer Engineering

Department: Electrical and Computer Engineering

School: School of Engineering

The undersigned certify that they have examined the final electronic copy of this thesis and approved it in Partial Fulfillment of the requirements for the degree of:

Master's of Science in Eng'g in the major of Computer Engineering

Thesis Advisor's Name: Dr. Harag Margossian

Signature: [redacted] Date: 25 / 5 / 2021 (Day / Month / Year)

Committee Member's Name: Dr. Raymond Ghajar

Signature: [redacted] Date: 27 / 5 / 2021 (Day / Month / Year)

Committee Member's Name: Dr. Dani Tannir

Signature: [redacted] Date: 25 / 5 / 2021 (Day / Month / Year)

LAU
الجامعة اللبنانية الأميركية
Lebanese American University

THESIS COPYRIGHT RELEASE FORM

LEBANESE AMERICAN UNIVERSITY NON-EXCLUSIVE DISTRIBUTION LICENSE

By signing and submitting this license, you (the author(s) or copyright owner) grants the Lebanese American University (LAU) the non-exclusive right to reproduce, translate (as defined below), and/or distribute your submission (including the abstract) worldwide in print and electronic formats and in any medium, including but not limited to audio or video. You agree that LAU may, without changing the content, translate the submission to any medium or format for the purpose of preservation. You also agree that LAU may keep more than one copy of this submission for purposes of security, backup and preservation. You represent that the submission is your original work, and that you have the right to grant the rights contained in this license. You also represent that your submission does not, to the best of your knowledge, infringe upon anyone's copyright. If the submission contains material for which you do not hold copyright, you represent that you have obtained the unrestricted permission of the copyright owner to grant LAU the rights required by this license, and that such third-party owned material is clearly identified and acknowledged within the text or content of the submission. IF THE SUBMISSION IS BASED UPON WORK THAT HAS BEEN SPONSORED OR SUPPORTED BY AN AGENCY OR ORGANIZATION OTHER THAN LAU, YOU REPRESENT THAT YOU HAVE FULFILLED ANY RIGHT OF REVIEW OR OTHER OBLIGATIONS REQUIRED BY SUCH CONTRACT OR AGREEMENT. LAU will clearly identify your name(s) as the author(s) or owner(s) of the submission, and will not make any alteration, other than as allowed by this license, to your submission.

Name: Youssef Shakrina

Signature: [redacted] Date: 08 / 04 / 2021
Day Month Year

LAU
الجامعة اللبنانية الأميركية
Lebanese American University

PLAGIARISM POLICY COMPLIANCE STATEMENT

I certify that:

1. I have read and understood LAU's Plagiarism Policy.
2. I understand that failure to comply with this Policy can lead to academic and disciplinary actions against me.
3. This work is substantially my own, and to the extent that any part of this work is not my own I have indicated that by acknowledging its sources.

Name: Youssef Shakrina

Signature: [redacted] Date: 08 / 04 / 2021
Day Month Year

ACKNOWLEDGMENT

This project was only possible due to the continuous support and supervision from my advisor Dr. Harag Margossian who provided valuable ideas and constructive feedback throughout the work of this thesis. Also, special thanks to the committee members, Dr. Harag Margossian, Dr. Raymond Ghajar, and Dr. Dani Tannir for their efforts in reviewing this thesis and evaluating the work.

A Stackelberg Game Inspired Model of Real-Time Economic Dispatch with Demand Response

Youssef Shakrina

ABSTRACT

Traditional electric power systems have several challenges in maintaining their reliability and being able to meet the demand of the consumers at peak hours. Additionally, environmental concerns may arise from several physical limitations in the network that would increase gas emission besides adding extra generation costs. With the advancements in the field of communications amalgamating in the power network, smart grids enable electric consumers to take part in changing the load profile through demand response (DR) programs to help overcome such challenges.

In some DR programs where the network's operators inform the consumers about the updated prices, predicting the change of the consumption pattern that will occur becomes arduous. Especially with the variety of electrical loads and their applications like the residential and industrial consumers and their different sensitivity to prices.

For optimal scheduling of generation units, this thesis presents a novel method for the operator to predict market prices and electrical loads under real-time pricing (RTP) DR program in a microgrid. Inspired by the Stackelberg game, the proposed model represents the interaction between the operator and the consumers. The model establishes simulated trading between the network's operator (leader) optimizing the generation cost and offering market prices to the customers (followers) who optimize their behavior. The interaction is formulated as a one-leader, N-follower iterative game where the optimization problems are solved using deterministic global optimization techniques. The proposed model considers a detailed representation of the industrial and residential loads. Simulations are performed on several microgrid systems where results show a significant improvement in the projected retail prices and electrical loads.

Finally, this thesis also examines the impact of energy storage systems (ESS) on the operation of an industrial facility in real-time demand response programs. A model is developed to optimally manage the energy storage and operation of the industrial load. Additionally, an approach to the sizing of the ESS is proposed. Stochastic modeling of electricity prices based on historical data is used to this end. The optimization models were tested on a generic industrial unit. Results show the benefits of ESS in increasing profit and highlight the impact of its installation cost on its feasibility.

Keywords: Demand Response, Economic Dispatch, Energy Storage, Game Theory, Optimization, Smart Grid, Stackelberg Game.

Table of Contents

Chapter **Page**

I. **Introduction** **1**

1.1 The Need for Smart Grids 1

1.2 Demand Side Management 2

1.2.1 Types of demand response programs 2

1.2.2 Implementation 4

1.3 Electricity Markets: Towards Liberalization 4

1.4 Problem Formulation 5

1.5 Thesis Organization 6

II. **Modeling Methods** **7**

2.1 Mathematical Optimization 7

2.1.1 Definition and types 7

2.1.2 DR modeling 8

2.2 Game Theory 8

2.2.1 Definition 8

2.2.2 Equilibriums and solutions 9

2.2.3 Game theory and DR 10

2.3 The Stackelberg Game 10

2.3.1 Definition 10

2.3.2 Stackelberg game and DR 11

2.4 Gaps and Contributions 12

III. **Leader's Strategies** **14**

3.1 Objective 14

3.2 Constraints 15

3.3 Market Price 16

IV. **Follower's Strategies** **17**

4.1 Residential Consumers 17

4.1.1 Objective function 17
4.1.2 Residential constraints 18
4.2 Industrial Consumers 19
4.2.1 Objective function 19
4.2.2 Industrial constraints 20
4.3 Iterative Stackelberg Game 22
4.3.1 System's flow 22
4.3.2 Discussion on convergence 23
V. **Simulations and Analysis 24**
5.1 Case Study 1: Simple Microgrid 24
5.1.1 Network description 24
5.1.2 Results and verification. 25
5.1.3 Discussion and analysis 30
5.2 Case Study 2: IEEE 24-RTS 31
5.2.1 Network description 31
5.2.2 Results 32
5.2.3 Discussion and analysis 34
5.3 Case Study 3: IEEE 123 Bus System 35
5.3.1 Network description 35
5.3.2 Results 36
5.3.3 Discussion and analysis 38
VI. **Elaborate Energy Management Model for the Industrial Consumers 40**
6.1 Energy Storage Applications 40
6.2 Related Work 40
6.3 Energy Management Model with ESS 41
6.3.1 Objective function 41
6.3.2 Constraints 41
6.4 Case Study 4 43
6.4.1 System description 43
6.4.2 Results 44

6.5 Energy Storage Sizing Model 45
6.6 Case Study 5 47
6.6.1 System description and results 47
6.6.2 Sensitivity analysis 49
6.6.3 Impact of considering several scenarios 49
VII. **Conclusion** **51**
References **53**
Appendix A: Simple Microgrid Network **58**
A.1 Network's Data 58
A.2 Residential Load Data 59
A.3 Industrial Load Data 59
Appendix B: IEEE 24 Bus RTS Network **60**
B.1 Network's Data 60
B.2 Residential Load Data 61
B.3 Industrial Load Data 62
Appendix C: Case Study 2 Results **64**
C.1 Generation Units 64
C.2 Industrial Load 65
Appendix D: IEEE 123 Bus System **68**
D.1 Network's Data 68
D.2 Residential Load Data 70
D.3 Industrial Load Data 70
Appendix E: Case Study 3 Results **73**
E.1 Generation Units 73
E.2 Industrial Load 74

Table of Figures

Figure 1 World Total Final Consumption (TFC) by Source 1
Figure 2 Industrial Load Scheme Number One 19
Figure 3 Case One System Schematic 24
Figure 4 Percentage Output of The Generation Sources: Case One-Initial Case 25
Figure 5 Percentage Output of The Generation Sources: Case One-Final Case 25
Figure 6 Market Prices in Different Iterations in Case One 26
Figure 7 Daily Residential Loads in Different Iterations: Case One 27
Figure 8 Daily Industrial Loads in Different Iterations: Case One 27
Figure 9 Updated 24 Bus RTS 32
Figure 10 Industrial Load Scheme Number Two 32
Figure 11 Market Prices in Different Iterations: Case Two 33
Figure 12 Daily Total Residential Loads in Different Iterations: Case Two 33
Figure 13 Daily Industrial Loads in Different Iterations: Case Two 34
Figure 14 Modified IEEE 123-Bus System 36
Figure 15 Market Prices Different Iterations: Case Three 36
Figure 16 Daily Residential Loads in Different Iterations: Case Three 37
Figure 17 Daily Industrial Loads in Different Iterations: Case Three 37
Figure 18 Schematic Diagram of Studied Industrial Load 43
Figure 19 Energy Demand and Energy Storage at Different Hours 45
Figure 20 Charging and Discharging of the ESS System 45
Figure 21 Expected Prices for Four New Scenarios 48
Figure 22 Percentage Output of The Generation Sources: Case Two-Initial Case 64
Figure 23 Percentage Output of The Generation Sources: Case Two-Final Case 64
Figure 24 Percentage Output of The Generation Sources: Case Three-Initial Case 73
Figure 25 Percentage Output of The Generation Sources: Case Three-Final Case 73

List of Tables

Table 1 Example of Non-Cooperative Game 9
Table 2 Machines On/Off Status: Case One-Final Case 28
Table 3 Number of Items in Buffers: Case Number- Final Case 29
Table 4 Iterations Output: Case One 30
Table 5 Iterations Output Case Two 34
Table 6 Iterations Output: Case Three 38
Table 7 Industrial Facility Parameters 43
Table 8 Day-Ahead Prices 44
Table 9 Upper Storage Capacity for Every Scenario 48
Table 10 Profit and Optimal Storage Capacity for Different ESS Installation Prices 49
Table 11 Conventional Generators Data: Case One 58
Table 12 Time-Varying Parameters: Case One 58
Table 13 Industrial Load Characteristics: Case One 59
Table 14 Machines Status: Case One-Initial Case 59
Table 15 Conventional Generators Data: Case Two 60
Table 16 Time-Varying Parameters: Case Two 60
Table 17 Line Data: Case Two 61
Table 18 Peak Consumption on Buses: Case Two 62
Table 19 Industrial Load Characteristics: Case Two 62
Table 20 Machines Status: Case Two-Initial Case 63
Table 21 Machines Status: Case Two-Final Case 65
Table 22 Number of Items in Buffers: Case Two-Final Case 66
Table 23 Fuel Based Generators Data: Case Three 68
Table 24 Time-Varying Parameters: Case Three 68
Table 25 Line Data: Case Three 69
Table 26 Peak Consumption on Buses: Case Three 70
Table 27 Industrial Load Characteristics: Case Three 71
Table 28 Machines Status: Case Three-Initial Case 72
Table 29 Machines Status: Case Three-Final Case 75
Table 30 Number of Items in Buffers: Case Two-Final Case 76

Chapter One

Introduction

1.1 The Need for Smart Grids

The world's requirements for energy have been rising throughout the years to meet humanity's need for industrial facilities, transportation usages, residential requirements, commercial services, and many more. This increase in energy consumption according to the international energy agency (IEA) is demonstrated in Figure 1 [1]. An increase of 113.26% in the world's total final consumption of energy has occurred between 1973 and 2018. Noticeably, the percentage of the demand for electrical energy among the demand for the total energy doubled in those years from 9.4% to 19.3%. Also, the total consumption of electrical energy has increased by more than four folds in that period [1].

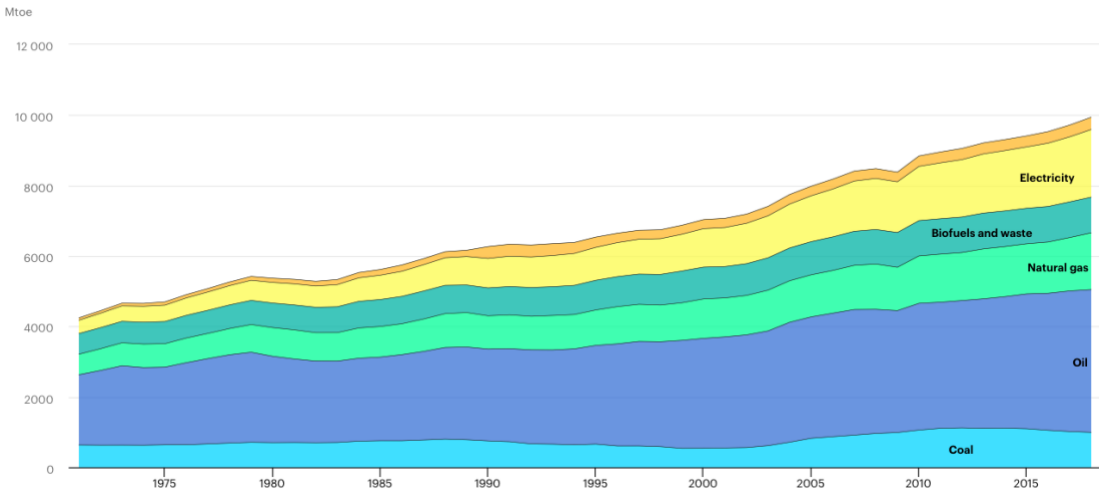

Figure 1 World Total Final Consumption (TFC) by Source

With great electric power demand, comes great responsibility. However, several incidents have shown how the traditional power grid did fail to provide service at peak hours. On July 12th 2004, the failure to supply high demand caused by a heatwave damaged the power system in Greece affected millions of citizens [2]. Similarly, on the cold day of February 2nd 2011, the increase in the electricity demand led to a blackout that lasted for eight hours in Texas [3]. Another reason for blackouts is the lag of communication between the network's operators. The famous 2006 "Europan

Blackout" was due to the late signaling to the transmission system's operator (TSO) that a powerline in Germany would be disconnected for other lines to handle the loads instead. The analysis for such an event was late and the system could not operate within the safety standards [4],[5]. As a result, 15 million houses lost electrical supply in 20 European countries and few north African countries [5]. Additionally, weather conditions and natural events may cause an interruption in the service [6].

To keep up with the growing demand, the transmission and distribution networks and equipment need to be replaced [7]. This physical upgrade in the network in addition to being expensive will reoccur more frequently in the future due to the ever-growing need for electricity. Moreover, environmental concerns are emerging because of the more emissions from the relatively cheap sources of electricity (coal, gas, and petrol) [7]. Such events and concerns are numerous and have occurred in the majority of nations, and they could have been prevented with better load management and faster and more reliable communication.

Bringing information and communication technologies (ICT) to the traditional grids for collecting data and communicating it between players involved in the grid, modernizes its capabilities to solve its reliability and control issues in a more autonomous way [7],[8]. Additionally, it enables the consumers to be active participants in the smart grid through demand side management (DSM) and demand response (DR) programs [8]. Demand response is defined as the incentives or tariff patterns that the power utility or network operators provide to the customers to alter their consumption schedule [8]. This shift in the demand would reduce the peak load and increase the consumption at a period that does not jeopardize the operation of the power network [8].

1.2 Demand Side Management

1.2.1 Types of demand response programs

DSM or DR programs can be generally classified into two main categories: incentive-based and price-based [8],[9].

In incentive-based programs, the electrical consumers are paid to decrease their load at peak hours. Incentives and their application can have different types as listed below [8],[9]:

- Direct load control (DLC): the utility has a control on certain appliances that can be turned off when necessary. In return for the inconvenience that occurred to the customers, they are paid incentives.
- Interruptible curtailment programs: the utility does not have direct control over the load, however, if the consumers agree to shed load when requested they earn incentives.
- Demand bidding programs: high load consumers (typically for loads >1MW) are offered these programs so they can profit from reducing their load for a certain bid price.
- Emergency demand reduction: incentives are paid on short notice when the network's reliability is jeopardized.

In price-based programs, the incentives for the customers to shift their loads are not payments, but the flat rate tariffs are replaced with prices that vary throughout the day or for different consumption levels. These prices may have several forms [8],[9]:

- Real-time pricing (RTP): the tariffs change at different intervals of time during the day. The updates may occur hourly, or even in shorter periods as in every 15 minutes for example.
- Time-of-Use (TOU): prices are not updated as often as the RTP. Typically, there may be three or four prices in a day representing the different on-peaks and off-peaks loads that can occur.
- Critical peak pricing (CPP): it follows the same structure as the TOU; however, it acts only during emergency events in the network.
- Inclining block rate (IBR): the prices do not change with time of the day as the previous DR programs, but with the consumption level. In this program, the tariff charged to the consumers is divided into two level rates. When their consumption exceeds a certain threshold, they get charged with the higher rate.

1.2.2 Implementation

All the aforementioned programs have been in use. Few examples of these employments are mentioned below:

- DLC programs were utilized by more than 200 utilities in the United States by the year 2012 where they pay bill credit incentives to the customers [10]. Typical electrical appliances controlled in the residential equipment are water heaters, pool pumps, and air conditioners but with a notification to the users on warm days [10]. Portland General Electric's (PGE) in the state of Oregon provides such programs where the incentives are lower rate structures for the customers who are willing to participate [11].
- Demand bidding programs: big utilities are offering such programs like "Southern California Edison", "CPower", "PG&E" [12]-[14].
- Price-based DR programs are more popular. TOU schemes are widely used in around 17 European countries, the USA, and India [15]. The dynamic pricing methods or RTP are also utilized in the USA [16] and several countries in Europe like Estonia, Sweden, U.K, etc. [15]. Similarly, the CPP programs are also adapted in those regions [15],[16].

1.3 Electricity Markets: Towards Liberalization

The electricity sector was under strict regulations in the past due to its significant role on society and the environment. These regulations were either in the form of public ownership of the electricity industry or different sorts of financial, environmental, or health controls over private ownership [17].

However, in recent decades, some countries in the European Union have deregulated the electricity industry through the concept of liberalization. These modifications were encouraged by the premise that privatization can improve economic efficiency and regulations can act as negative incentives for the operation of industries [17]. As a result, the state-owned sector was divided into different firms to handle the generation of power, its transmission, and distribution [17]. This being said, several opinions were against these theories because of the fear of exploiting the market power. However, the current status of most of the electricity industry in leading countries is either privatized or state-owned with minimal regulations, for what is believed to lead to lower prices and high efficiency [17].

1.4 Problem Formulation

As mentioned before, the change of the consumption patterns and the intelligence added to the grid for faster communication have been the interests of researchers to further enhance the performance of the power grid. Benefits of DR for the power system include: 1) peak load shaving [18]-[20], 2) reducing emissions [21]-[23], 3) supporting renewable energy integration [24], 4) enhancing the reliability of the network [25],[26], and 5) reducing power losses in the transmission lines [27]. Consumers, on the other hand, benefit from 1) primarily cost-saving, as well as, 2) greater engagement in the operation of the system.

The different types of objectives in DR programs and the different kinds of consumers and loads make the need to model the behavior of the participants, programs, and systems essential. Many techniques have been proposed to make the most out of DSM. Optimization methods were utilized in addition to game theory models to represent the interests of the supply side, the demand side, DR programs, network constraints, emission impacts, and more.

This thesis presents a new model to represent the interaction between the network's operator (supply-side) and different types of consumers (demand-side) under the RTP program. The proposed model comes around the gap in the previous models by being more realistic and more comprehensive. The contribution of this model, techniques used, and simulations will be detailed throughout the thesis.

The new model presented is inspired by a game theory model and several optimization techniques. It does not only consider the detailed representation of the residential and industrial consumers, but it also considers the several limitations of the operator.

Furthermore, more investigations on the industrial consumers' model are performed by developing a model for energy storage system (ESS) management and sizing in day-ahead real-time pricing markets.

1.5 Thesis Organization

In Chapter Two, the mathematical tools for modeling in this field will be represented, in addition to their applications in the literature. This chapter highlights the contribution of the proposed model.

In Chapter Three, the optimization model of the operator is explained: the objective, the constraints, and the limitations. In Chapter Four, the detailed optimization models of the residential and industrial customers are presented. Moreover, the iterative game approach proposed in this work is clarified.

In Chapter Five, simulations of the proposed methods are carried out on several networks. Their outcomes are analyzed and compared to other scenarios to illustrate the significance of the work.

In Chapter Six, the ESS management models and sizing approaches for the industrial loads are presented. Two case studies are performed to analyze the validity of these models.

Chapter Seven concludes the thesis and the work. Finally, additional information regarding the test systems and their outcome are represented in the Appendices.

Chapter Two

Modeling Methods

This chapter explains the mathematical concepts that will be used throughout the thesis to model the interactions in the smart grid. Moreover, it clarifies the contributions of the proposed model.

2.1 Mathematical Optimization

2.1.1 Definition and types

Optimization is a mathematical model to express an objective with mathematical symbols. The goal behind this model is to make the best of the system (e.g. minimizing losses, maximizing profit). The generic idea is to write the targeted aim in an expression with *decision variables* that give it its value. This aim is the *objective function* that will be either maximized or minimized. The limitations of the decision variables are the *constraints* that prevent the maximization/minimization of the objective function from being +infinity/-infinity [28]. Generally, an optimization problem is expressed as:

max/min objective function

subject to: constraint 1

constraint 2 …

Not all optimization models are created equal. The nature of the variables (integers or real numbers), the type of the objective function or the constraints (linear, convex, non-linear...) leads to diverse methods to find the optimal solution with different difficulties and computational burdens [28]. Some of the techniques presented are: Linear Programming (LP), Mixed-Integer Programming (MIP), Non-linear Programming (NLP), Dynamic Programming (DP)… Heuristic and meta-heuristic techniques have been proposed to search for a sufficiently good solution given the computation limitations [28].

2.1.2 DR modeling

In the context of smart grids, the previously mentioned techniques are widely exploited to model the behavior of the customers upon the change of the prices or the incentives paid. Classic optimization problems modeled real-time pricing (RTP) using demand elasticity, defined as the sensitivity of customers' response to the change in price [29],[30]. In [29], demand elasticity is used to maximize social welfare, whereas in [30], the authors minimize the cost of generation. More detailed modeling of DR with a focus on scheduling or controlling specific appliances with the help of smart meters is also considered. In [31], the authors consider direct load control of specific buses to decrease losses in the system. The prices of the day-ahead market are assumed unknown and are predicted by forecasting modules. Optimally scheduling residential, commercial, and industrial equipment in the RTP program is considered in [32], while minimizing the squared of differences between the actual and the desired loads. These models are solved using deterministic global optimization including LP, NLP, and mixed-integer nonlinear programming (MINLP) or using heuristic optimization when dealing with a very large number of variables [32].

With the nature of conflicts and different interests among several players in the smart grid, the traditional optimization problems become limited in the representation of these players. "Game Theory" came as a nifty mathematical tool to model such interactions in the previous century.

2.2 Game Theory

2.2.1 Definition

Modern Game Theory was first proposed in 1944 by John von Neumann and Oskar Morgenstern in an attempt to model the economic behavior of individuals or companies. The key idea is to model the interaction among individuals or players that are bounded with specific rules to dictate the moves and the outputs of those players [33]. Therefore, game theory is a model for almost all social interaction of aware individuals willing to enhance their utility [33]. The moves of the players are noted as *strategies* and the outcome of their moves is called *payoff* [28].

The different interactions lead to different types of games [28],[33]:

- Co-operative & non-cooperative games: the difference is whether the players have a binding commitment between each other (as in the case of co-operative games) that can limit their payoff.
- Zero-sum game: the payoff of each player is balanced by those of other plays. In short, the sum of those payoffs of each move should be zero.
- Simultaneous & dynamic games: In simultaneous games, the players move at the same time or do not know what other players have already played. Dynamic games are when each player knows what the other players have already performed, and accordingly, they can make informed decisions.

In addition to other forms of games like infinitely long games, Stackelberg games, symmetric & asymmetric games…

2.2.2 Equilibriums and solutions

To solve a game model means to come up with a reasonable case from the strategies of the players, that makes both players satisfied with the outcome and have no incentives to deviate. Because of the nature of unwillingness to deviate from the solution, the term solution is often interchangeable with the term *equilibrium* [33].

Nobel prize winner Sir John Nash proposed a so-called *beautiful idea* to solve non-cooperative games. A game in Table 1 is expressed in the *matrix form* (or the *normal form*), player 1 and player 2 have two strategies to choose from R1, R2 and C1, C2 respectively. Nash proposed to solve such a game, the best reply for the opponent's strategy should be considered. In Table 1, the best response for strategy C1 by player 2, is for player 1 to go with R1 because 10>9. Therefore 10 is denoted with $^{+}$. Likewise, the best response for strategy R1 by player 1, is for player 2 to play C2 because 5>4. Hence it is denoted with $^{-}$. Following this logic for all strategies shows that the only coincidence between both best reply strategies is (R1,C2) and hence the *Nash equilibrium* is found [33].

Table 1 Example of Non-Cooperative Game

	C1	C2
R1	$^{+}10,4$	$^{+}1,5^{-}$
R2	$9,9^{-}$	0,3

The mentioned example is only a simple game, but it shows the general idea behind game models and how the player will decide depending on the different interests of other players. Interestingly, with mixed strategies (i.e., each player can choose a move with a certain probability) at least one Nash equilibrium exists [33].

Other solutions have been proposed throughout the past century to solve the different kinds of games. *Backward induction* proposes that to solve dynamic or sequential games one should start thinking backward to find the sequence of optimal strategies. In the *forward induction* technique, how the strategy played now will cause inference to other players in the next steps is considered. *Nash solution* (different from Nash equilibrium) and *Rubinstein's solution* methods were proposed to solve bargaining games [33].

2.2.3 Game theory and DR

Game theory was proposed as a convenient technique to represent the different interests of players in the smart grid and to better model DR. In [34], a model was established to reduce the peak-to-average ratio by sending real-time price signals from the power supplier to customers who are aiming to maximize their value. The authors in [35] build a model where social welfare is maximized in the RTP scheme, with consumers declaring their energy demand information. The payoff function (utility) is designed to be concave to better reflect the interests of customers. The Nash equilibrium and competitive equilibrium were analyzed. The authors in [36], propose a model to set TOU prices to maximize the profit minus the satisfaction cost of the company while consumers maximize their utility function. The Nash equilibrium was obtained using backward induction.

2.3 The Stackelberg Game

2.3.1 Definition

The Stackelberg concept was introduced in 1934 in an attempt to model the interaction in markets where some firms dominate others. The competition starts with the dominant firm or the *leader* announcing its strategy and the other firms or *followers* reacting to it. With both companies being rational and the leader having perfect knowledge of the other's objective function, the leader's best strategy is found with

anticipation of the follower's optimal responses [37]. Typically, the solution is found using standard mathematical calculus.

Later on, the Stackelberg concept was added to the sequential multi-level dynamic games. In such cases, the leader has the upper hand in the current state of the sequential game. Stackelberg equilibrium (S.E) could be obtained through backward induction. However, if the leader has the power to set strategies first throughout the whole process, then finding the global Stackelberg solution becomes difficult because the solution sets become very large, almost infinite [37]. Lately, the amalgamation of Stackelberg games with other modeling concepts continued.

2.3.2 Stackelberg game and DR

For improved modeling of the interactions between the customers and the utility, operators, retailers, or energy centers, the Stackelberg game form is exploited. In a Stackelberg game, the utility or operator is the leader who first sets the price of electricity for each period, the consumers are followers who act upon the leader's strategy and set their optimal strategies [38]-[41]. The authors in [38] model the relationship between a retailer and N residential customers who announce their power consumption updates. The retailer aims to maximize his/her profit while the customers intend to maximize the quality of their power consumption. Reference [38] proposed a distributed algorithm to solve the consumers' model. Reference [39] utilized the Stackelberg game to model the interaction between retailers wanting to maximize their profit and customers trying to minimize their bill costs. The leader's optimization problem was solved using a genetic algorithm while the follower's linear programming problem was solved analytically. The prices are announced through smart meters then customers react accordingly by automatically rescheduling appliances. In [40], the model aims to find the effect that DR can bring to generation companies and consumers in the smart grid using the Stackelberg framework, by observing the behavior of the consumers optimally adjusting their load to the new prices. The leader tries to solve the economic dispatch problem and then submit the bid to the wholesale market. Next, the operator finds the optimal prices. With the day ahead prices sent to the customers, they maximize their utility accordingly. Reference [40] shows that day ahead RTP does not always lead to lower generation costs. The authors in [41] consider the virtual (non-physical) power trading model between the energy management center and devices to achieve optimal load control of the load. The leader maximizes the

benefit from selling electricity while the devices aim to minimize the monetary cost and the dissatisfaction from shifting the appliances' schedule. Each optimization problem is solved and then the outputs are used for the other model in an iterative process until the S.E is achieved.

2.4 Gaps and Contributions

The model presented in this thesis is intended to represent the case in electricity markets in a very realistic and comprehensive fashion.

The consumers are diverse, and their consumption patterns will differ under DR programs. However, in the existing models, a tradeoff occurs either in not representing all types of customers [19],[20],[25],[31],[34],[38] or in simplifying the representation of industrial loads [27],[32],[35],[36].

The generation capacity and the physical constraints of the grid are essential and can cause major changes in the prices. Despite this, as a simplification, some of the models ignore power flow [18]-[21],[30],[33],[35].

Additionally, in the game theory approach, customers are assumed to have perfect knowledge [36],[40] and to be capable of making collective decisions and thus impacting the electricity/incentive price [35],[38],[40]. This may be true if a direct load control DR program is utilized, however, in RTP, each consumer does not alter his/her consumption by coordinating with others. Rather he/she reacts to the prices as an individual household, company, or an industry. Also, each consumer is not aware of the utility's conditions and generation capacity, and thus no knowledge of how the change of the consumption will affect the market prices.

The work in this thesis builds a Stackelberg game model to represent the interaction between the network operator and the variety of consumers. The model is from the perspective of the microgrid's operators who are price setters in the market. A microgrid is considered because the knowledge of consumers' parameters cannot be generalized to bigger grids. Residential and industrial consumers are simulated by the operator as price takers. This simulated power trading scheme allows the operator to better predict consumer response to the RTP program and, consequently, to better optimize the microgrid's economic dispatch.

The proposed modified Stackelberg game is then defined as follows: the leader (operator) declares the electricity prices after an initial economic dispatch. The "simulated" followers (residential and industrial consumers) react to the new prices by optimizing their load. The operator then re-calculates the new prices and sends them to the followers. The model keeps on iterating until convergence within a predefined threshold.

The major contributions of the thesis are that it presents a non-compromising game model to describe the interests and the interactions between the operator and the customers, and it further investigates the impact of DR on optimal economic dispatch. Compared to most related works in literature, the presented approach is characterized by: 1) detailed modeling of residential and industrial consumers without compromising the complexity of the modeled power system (by virtue of the presented iterative approach), 2) more accurate representation of consumers as price takers without the ability of collective decision making to affect electricity prices (as opposed to the traditional Stackelberg game approach), and 3) guaranteed convergence of the model by controlling the threshold of load changes and prices between iterations.

In the following chapter, the operator side of the Stackelberg game is discussed and modeled.

Chapter Three

Leader's Strategies

In this chapter, the optimization problem for the operator is discussed. The objectives and constraints are modeled and analyzed.

3.1 Objective

In a grid, the role of the operator is to meet the electrical demand with the minimum generation costs possible. The operator has to successfully schedule the generating units while satisfying the technical and physical limitations of the network [42]. This process is known as the *economic dispatch*. The power network is made up of several *nodes* or *busses*, where power lines are connected, and certain generations and loads may be included.

The goal of the microgrid operator in an economic dispatch problem is to minimize its total costs including generation costs and purchase costs from the main grid. The objective function *OF1* is thus given as follows:

$$\min OF1 = \sum_{t=1}^{T}\sum_{i=1}^{I} C_i\left(P_{i,t}\right) + \sum_{t=1}^{T}\sum_{i=1}^{I} C_i\left(Pr_{i,t}\right) \quad (1)$$

Where $P_{i,t}$ is the generator's active power output on bus *i* in period *t*, $Pr_{i,t}$ is the transferred power given on bus *i* in period *t*, and sets I and T are the sets of network buses and time-periods respectively.

The generation cost is given as:

$$C_i\left(P_{i,t}\right) = a_i P_{i,t}^2 + b_i P_{i,t}, \qquad t \in T; i \in I \quad (2)$$

Where a_i and b_i are generation cost coefficients of the unit at bus *i*.

The cost of purchasing from the main grid is given as:

$$C_i\left(Pr_{i,t}\right) = \tau Pr_{i,t}, \qquad t \in T; i \in I \quad (3)$$

Where τ is transferred power marginal price.

3.2 Constraints

Line Limits: Real and reactive powers between buses *i* and *j* in period t ($P_{ij,t}$, $Q_{ij,t}$) are given as:

$$P_{ij,t} = \frac{|V_{i,t}|^2}{Z_{ij}}\cos(\gamma_{ij}) - \frac{|V_{i,t}||V_{j,t}|}{Z_{ij}}\cos(\gamma_{ij} + \delta_{i,t} - \delta_{j,t}), t \in T; i, j \in I \quad (4)$$

$$Q_{ij,t} = \frac{|V_{i,t}|^2}{Z_{ij}}\sin(\gamma_{ij}) - \frac{|V_{i,t}||V_{j,t}|}{Z_{ij}}\sin(\gamma_{ij} + \delta_{i,t} - \delta_{j,t}) - \frac{bsh_{ij}|V_{i,t}|^2}{2}, \quad t \in T; i, j \in I \quad (5)$$

Where Z_{ij} is impedance magnitude of branch connecting bus *i* to *j*, γ_{ij} impedance angle of branch connecting bus *i* to *j*, bsh_{ij} is the charging susceptance of the line connecting buses *i* and *j*, and $V_{i,t}$ and $\delta_{i,t}$ are the voltage magnitude and the phase angle of a bus *i* in period *t* respectively.

The total apparent power through a line ($S_{ij,t}$) at any given time cannot exceed the capacity of the line ($S_{ij,max}$):

$$S_{ij,t} = \sqrt{{P_{ij,t}}^2 + {Q_{ij,t}}^2} \leq S_{ij,max}, \quad t \in T; i, j \in I \quad (6)$$

Voltage and phase limits: $V_{i,t}$ and $\delta_{i,t}$ must satisfy power quality and reliability constraints:

$$0.9 \times \text{Vbase} \leq V_{i,t} \leq 1.1 \times \text{Vbase}, \quad t \in T; i \in I \quad (7)$$

$$\frac{-\pi}{2} \leq \delta_{i,t} \leq \frac{\pi}{2}, \quad t \in T; i \in I \quad (8)$$

$$\delta_{slack,t} = 0, \quad t \in T \quad (9)$$

Where *Vbase* is the base voltage of the system.

Power balance: in every period *t*, the sum of generated power on bus *i* plus the power purchased or sold from the main grid should be equal to demand on the bus, in addition to the power in the lines connected to it.

$$P_{i,t} + Pr_{i,t} = \sum_{j=1}^{I} P_{ij,t} + Pl_{i,t}, \quad t \in T; i \in I \quad (10)$$

$$Q_{i,t} + Qr_{i,t} = \sum_{j=1}^{I} Q_{ij,t} + Ql_{i,t}, \qquad t \in T; i \in I \tag{11}$$

Where $Pl_{i,t}$ and $\mathrm{Q}l_{i,t}$ are the real and reactive loads on bus *i* in period *t*. A constant power factor is considered for the residential and industrial loads and the transferred power.

Generation capacity: The generators have upper $(P_{i,max}, Q_{i,max})$ and lower $(P_{i,min}, Q_{i,min})$ generation limits. There is also a limit for how much power can be transferred from and to the microgrid $(Pr_{i,min}, Pr_{i,max})$. The constraints are expressed in (12) →(14).

$$P_{i,min} \leq P_{i,t} \leq P_{i,max}, \qquad t \in T; i \in I \tag{12}$$

$$Pr_{i,min} \leq Pr_{i,t} \leq Pr_{i,max}, \qquad t \in T; i \in I \tag{13}$$

$$Q_{i,min} \leq Q_{i,t} \leq Q_{i,max}, \qquad t \in T; i \in I \tag{14}$$

Ramping limits: generators cannot shift their output by a large amount directly, they have to abide by lower (DR) and upper (UR) ramping limits.

$$-\mathrm{DR} \leq P_{i,t+1} - P_{i,t} \leq \mathrm{UR}, \qquad t \in T; i \in I \tag{15}$$

3.3 Market Price

After the model is solved, the market price in period *t* is defined as the marginal cost of generation of the most expensive unit. Therefore, the market price at period *t, $Price_t$,* is the marginal cost of the most expensive operating unit at that period.

$$Price_t = \max\left(\frac{dC_i(P_{i,t})}{dP_{i,t}}, \frac{dC_i(Pr_{i,t})}{dPr_{i,t}}\right), \qquad t \in T; i \in I \tag{16}$$

This price will be the only information from the leader that followers will have to play their strategies. In the next chapter, the followers' objectives, constraints, and optimization problems will be modeled.

Chapter Four

Follower's Strategies

Electricity consumers are divided into residential, commercial, and industrial loads. Residential loads are characterized by high responsiveness due to their sheddable, non-sheddable, and shiftable loads [9]. Commercial loads are the least responsive since they operate in fixed hours per day and their load is not flexible [9]. Finally, industrial loads involve independent machines operating in manufacturing lines, making their DR model more complex [43].

In the proposed model, the operator of a microgrid can obtain the parameters of the residential and industrial customers by deducing them from historical data or by requesting the information of the devices and the manufacturing process as a condition for participating in the DR program, or for connecting to the grid. This is a reasonable assumption since participation in the DR program is optional and the information will be used to improve the operation of the system and enhance the experience and interests of the consumers. Commercial loads are ignored in this thesis as their interaction with demand response is minimal.

4.1 Residential Consumers

4.1.1 Objective function

The main objective of residential customers is to utilize electrical energy in a cost-effective way. A typical way to model such interest is to build a utility function, normally a concave function, that is dependent on price. In this thesis, the proposed game represents the payoff of the residential consumers as an electric bill to be minimized, however, the bounds on the change of consumption are modeled as constraints. Therefore, the objective function of residential consumers *OF2* is:

$$\min OF2 = \sum_{t=1}^{T} \sum_{i=1}^{R} Price_t \times (Pl_{i,t} + Xr_{i,t}) \qquad (17)$$

Where $Xr_{i,t}$ is the load that can be reduced or increased in period t and R is the subset of buses with residential loads.

The residential load is divided into non-sheddable loads that cannot be turned off or rescheduled, sheddable loads that consumers can give up on using, and shiftable loads that consumers can stop using on certain hours and reuse later [9]. These will be modeled as constraints to mimic how much customers value electrical energy.

4.1.2 Residential constraints

Shedding limits: y% of the total load is sheddable in one day. These reflect the appliance that residential customers are willing to give up their consumption as air compressors, battery chargers, television… So, the total new load in one day can go down to (100-y)% of the initial total load of the day, as shown in (18).

$$\sum_{t=1}^{T}(Pl_{i,t} + Xr_{i,t}) \geq \left(1 - \frac{y}{100}\right)\sum_{t=1}^{T} Pl_{i,t-initial}\,, \qquad i \in R \tag{18}$$

Where $Pl_{i,t\text{-}initial}$ is the initial active power demand at bus *i* in period *t*.

Shifting limits: in a period *t*, a certain percentage of the load can be changed. These reflect appliances that can be rescheduled, like dishwashers or dryers, in addition to their percentage of the total load during hours of the day. The residential consumers' loads are more flexible during the daytime and less flexible after midnight. Therefore the change of the load ($Xr_{i,t}$) is bounded between a percentage ϵ_t of the initial load as shown in (19).

$$-\epsilon_t \mathrm{Pl}_{\mathrm{i,t-initial}} \leq \mathrm{Xr}_{\mathrm{i,t}} \leq \epsilon_t \mathrm{Pl}_{\mathrm{i,t-initial}}, \qquad \mathrm{t} \in \mathrm{T}; \mathrm{i} \in \mathrm{R} \tag{19}$$

Non-sheddable loads: in a period *t*, the load has to be greater than z% of the initial load. These reflect appliances that customers are willing to utilize no matter how much prices are high. Typically, these appliances consume high power like refrigerators, heaters in cold weather, total lighting loads…

$$\mathrm{Pl}_{\mathrm{i,t}} + \mathrm{Xr}_{\mathrm{i,t}} \geq \frac{\mathrm{z}}{100}\mathrm{Pl}_{\mathrm{i,t-initial}}, \qquad \mathrm{t} \in \mathrm{T}; \mathrm{i} \in \mathrm{R} \tag{20}$$

RTP constraint: the market considered is not a day-ahead price but a real-time market. Hence, it is a fair assumption that customers cannot shift their loads to earlier times. This can be modeled by making the sum of the new load up to every period *t* less than the initial load up to that period.

$$\sum_{t=1}^{n}(Pl_{i,t} + Xr_{i,t}) \leq \sum_{t=1}^{n} Pl_{i,t-initial}\,, \qquad n \in T, i \in R \tag{21}$$

4.2 Industrial Consumers

4.2.1 Objective function

The industrial load is a set of machines operating to give items that are fed to the next machine until the final product is manufactured. [43] and [44] modeled a general form of industrial behavior. Unlike residential consumers, shedding a machine could affect the whole consumption pattern throughout the day due to interconnections of the appliances. The model in this thesis is adapted from [43]. As mentioned earlier, it is assumed that this information is made available to the operator at the time of connection.

Figure 2 shows an example of an assembly line of industry. The rows "*r*" are numbered from 1→ S, and each row has M_r columns "*c*". The assembly line combining other lines is indexed r=0 and has M_0 columns. Each machine is drawn as a square followed by a buffer for storage labeled as a circle.

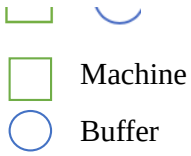

Figure 2 Industrial Load Scheme Number One

For more compact equation representation, the dimension considering the network buses with industrial loads (set D) is omitted in the below model of the industrial load.

The objective of the industrial consumers is to maximize their profit which is the revenue they gain from selling the assembled products minus the costs of the material needed for manufacturing and the electricity bill. Therefore, the objective function to maximize by the industrial consumers *OF3* is:

$$\max OF3 = KsB_{0M_0t_{24}} - \sum_{t=1}^{T}\sum_{r=1}^{S} KP_r\beta_r n_{r1t} - \sum_{t=1}^{T}\sum_{r=0}^{S}\sum_{c=1}^{M_r} Price_t x_{rct} Eon_{rc} \tag{22}$$

Where *Ks* is the price of the product manufactured in the market. $B_{oM_0t_{24}}$ is what the machines produced in a day that is stored at the very end buffer at the end of the day. KP_r is the price of the material purchased to operate the machines in the first columns. β_r is the number of these items needed to manufacture one product by a machine. x_{rct} is a variable indicating the on/off status of a machine in row r and column c in a period *t*. Eon_{rc} is the power needed for each machine when it is operating.

4.2.2 Industrial constraints

The following constraints to model the behavior are used in [43]. The scheduling horizon of a day is divided into *Ts* slots. Here the day is divided into 24 slots.

Machine's output quantity: Each machine can generate *n* items in a time slot *Ts*. CT_{rc} is the cycling time of a machine. The number of outputs of each machine in period *t* (n_{rct}) is expressed in (23).

$$n_{rct} = \frac{T_s}{CT_{rc}} x_{rct} \quad , t \in T; r = 0, \dots, S; c = 1, \dots, M_r \tag{23}$$

For example, if a machine r1.c1 is turned on, with Ts = 60 mins and CT_{rc} = 50s, then machine r1.c1 produces 60*60/50 =72 items per hour.

Buffer storage: After each machine, there is a buffer B_{rc} to store the manufactured product that will be fed to the next machine. The buffer storage at given period *t* (B_{rct}) is given by:

$$B_{rct} = B_{rc(t-1)} + n_{rct} - \alpha_{rc} n_{r(c+1)t}, \quad t \in T; r = 0, \dots, S; c = 1, \dots M_r - 1 \tag{24}$$

$$B_{rct} = B_{rc(t-1)} + n_{rct} - \alpha_{rc} n_{01t}, \quad t \in T; r = 1, \dots, S; \mathrm{c} = M_r \tag{25}$$

$$B_{rct} = B_{rc(t-1)} + n_{rct}, \quad t \in T; r = 0; \mathrm{c} = M_0 \tag{26}$$

Where α_{rc} is a coefficient describing the number of parts from B_{rc} that is necessary for the machine after it to produce one part.

Equation (24) shows that the items in a buffer in period *t* equals the number of items in the previous time slot in addition to what is produced and added to it at the current time slot, minus the parts which are taken for the next machine to operate. This

equation applies to the buffers in all the rows except the last buffer in them since there are no machines left in the same row.

Equation (25) describes the behavior of the machines at the end of the non-assembly lines, where their outputs are used by machine r0.c1. It follows the same logic as (24), however, the outputs of those machines are fed to r0.c1.

Equation (26) describes the behavior of the last buffer where it accumulates all the final products.

Machine operation conditions: The machine operates if and only if the previous buffer has enough items (except the first machines in every line):

- If a buffer feeding a machine is empty ($B_{rc(t-1)} = 0$), then this machine in the next period is off ($x_{r(c+1)t} = 0$).
- If a buffer feeding a machine is not empty ($B_{rc(t-1)} > 0$), then this machine in the next period can operate ($x_{r(c+1)t} > 0$).

The relation in (27) satisfies these conditions.

$$x_{r(c+1)t} \leq B_{rc(t-1)}, \qquad t \in T; r = 0, \dots, S; c = 1, \dots, M_r - 1 \tag{27}$$

The first machine at the beginning of the assembly line (r = 0) does not operate if the buffers at the end of the rows 1→S are empty, as modeled in (28). It follows the logic in (27).

$$x_{01t} \leq B_{rc(t-1)}, \qquad t \in T; r = 1, \dots, S; c = M_r \tag{28}$$

Buffer storage limits: The buffers have upper limits of storage capacity (CAP_{rc}) and naturally cannot have negative storage.

$$0 \leq B_{rct} \leq CAP_{rc}, \qquad t \in T; r = 0, \dots, S; c = 1, \dots, M_r \tag{29}$$

Full buffer blockage rule: Finally, if the buffer is full, its corresponding machine will be blocked from operating: If a buffer feeding a machine is full ($B_{rc(t-1)} = CAP_{rc}$), then the corresponding machine in the next period is off ($x_{rct} = 0$).

Equation (30) satisfies this condition.

$$x_{rct} \leq CAP_{rc} - B_{rc(t-1)}, \qquad t \in T; r = 0, \dots, S; c = 1, \dots, M_r \tag{30}$$

RTP constraint: like residential loads, industrial loads are assumed to not shift their loads to earlier in the real-time pricing market as expressed in (31). It follows the logic in (21).

$$\sum_{t=1}^{n}\sum_{r=0}^{S}\sum_{c=1}^{M_r} x_{rct,i} Eon_{rc,i} \leq \sum_{t=1}^{n} Pl_{i,t-initial}\,, \qquad n \in T, i \in \mathrm{D} \tag{31}$$

Where *D* is the subset of buses with industrial loads.

Non-binary operation: B_{rct} and n_{rct} are obviously positive integers. In [43], x_{rct} is a binary variable indicating if the machine is strictly on/off. In this thesis, to model a large power consumption machine that operates in non-discrete mode, x_{rct} is defined as a variable bounded between 0 and 1.

In the case of the elastic operation mode, ramping limits (ψ) are set:

$$-\psi \leq x_{rct} - x_{rc(t-1)} \leq \psi, \qquad t \in T; r = 0, \dots, S; c = 1, \dots M_r \tag{32}$$

4.3 Iterative Stackelberg Game

4.3.1 System's flow

With the well-defined leader's and followers' strategies and objectives, the Stackelberg game can be modeled.

A game is played between the operator as a leader and the residential and industrial customers as followers. The operator calculates the economic dispatch for an initial load of customers not participating in DR programs. For that, he/she will minimize (1) subject to (2) → (15) using NLP. Then, the market price is found with (16).

Next, the system starts iterating by performing the following:

The operator will try to predict the behavior of the customers and how they will shift their loads with the updated prices when participating in the RTP DR program considering that:

1) The residential customers will minimize (17) subject to (18) →(21) using NLP. The new residential load is then calculated as:

$$Pl_{i,t} = Pl_{i,t} + Xr_{i,t}\,, \qquad t \in T; i \in R \tag{33}$$

2) Industrial customers will maximize (22) subject to (23) → (31) and (32) (for non-discrete manufacturing mode) using MIP. The new industrial load is then calculated as:

$$Pl_{i,t} = \sum_{r=0}^{S} \sum_{c=1}^{M_r} x_{rct,i} Eon_{rc,i}\,, \qquad t \in T; i \in \mathrm{D} \tag{34}$$

If both the residential and industrial load do not change their loads, *i.e.*, every $Xr_{i,t}$ is 0 and all x_{rct} are the same as the previous iteration, then the model stops. If not, another iteration is performed.

3) The operator will re-find the economic dispatch and new prices will emerge.

4.3.2 Discussion on convergence

Theorem 1 has been previously proposed for the existence of a unique S.E [41],[45].

Theorem 1: For the proposed one-leader, *N*-follower Stackelberg game, a unique SE exists between the operator and the customers if the following conditions are satisfied:

1) The strategy sets of the leader and the followers are nonempty, compact, and convex.
2) Each customer has a unique optimal strategy solution as a best response for the operator's strategy.
3) The operator has a unique optimal strategy solution as a best response for the follower's best strategies.

The non-convex AC power flow equations in the leader's model [46], in addition to the integer variables in the industrial load follower's model, make the analytical proof of the existence of the Stackelberg equilibrium arduous.

To ensure convergence of the iterative process of the proposed modified Stackelberg approach, the following conditions are considered:

1) If the followers do not change their consumption from the previous iteration, or the change in load is within a specified threshold, $r_{L,}$ iterations stop.
2) If the followers have more than one unique optimal response for the leader's strategy, then the same electric prices would have different optimal strategies for the customers. If two consecutive iterations lead to the same real-time prices, or the change in prices is below a specified threshold, r_P, the iterations stop.

Chapter Five

Simulations and Analysis

Three case studies that verify the feasibility of the proposed game model are carried out in this chapter. Their results are further analyzed and discussed. The handy tool to model and solve complex optimization problems: General Algebraic Modeling Language (*GAMS*) is used to solve all the optimization models in this thesis.

5.1 Case Study 1: Simple Microgrid

5.1.1 Network description

The purpose of studying this basic system is to analyze the details of every element of the grid more easily, instead of focusing only on the effect on the market. The studied system is adapted from [47]. An industrial load is added to the found residential consumers. Extra two conventional generators are installed to supply the new demand. As shown in the schematic in Figure 3 [48] and Appendix A, the system also consists of PV and wind energy sources in addition to a connection to the main grid to sell and purchase power. No power flow analysis or reactive power equations are considered in this simple case, and a discrete industry manufacturing process is studied.

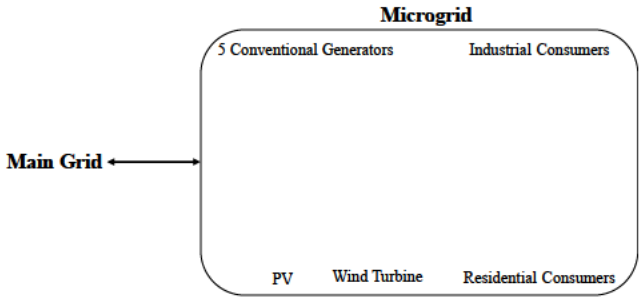

Figure 3 Case One System Schematic

There are no network busses in this system, so the residential loads are lumped together. This means the dimension considering busses (set I) is eliminated in the equations. The generation capacities, costs, and residential load data are listed in detail in Appendix A. The industrial manufacturing scheme is shown in Figure 2. The initial machines' status and manufacturing costs and power demand are shown in Appendix A as well.

For this simplified case study, the operator minimizes (1) subject to (2), (3), (10), (12), (13), and (15). The followers minimize (17) subject to (18)→(21) for residential customers and maximize (22) subject to (23) → (31). Set I dimension of the constraints and power flow analysis equations are removed.

5.1.2 Results and verification.

This model is tested on GAMS using the SCIP solver, and it took five iterations to converge. This means in the fifth iteration the customers did not change their load, so the model stopped.

The simulation shows the following results:

Generating units: The output of the power sources is the main decision for the operator to make. The percentage generation output of the units for the initial loads and last loads are shown in Figure 4 and Figure 5 respectively.

- Initial load dispatch:

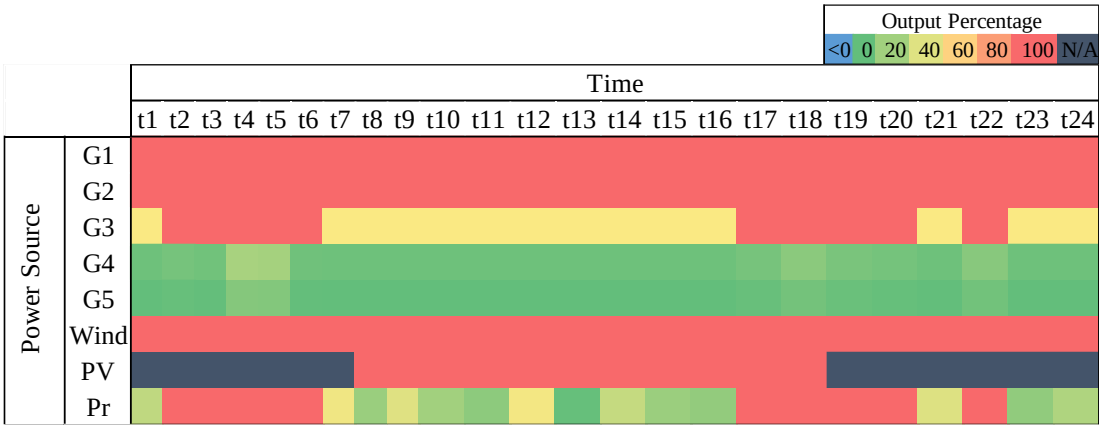

Figure 4 Percentage Output of The Generation Sources: Case One-Initial Case

- Final load dispatch:

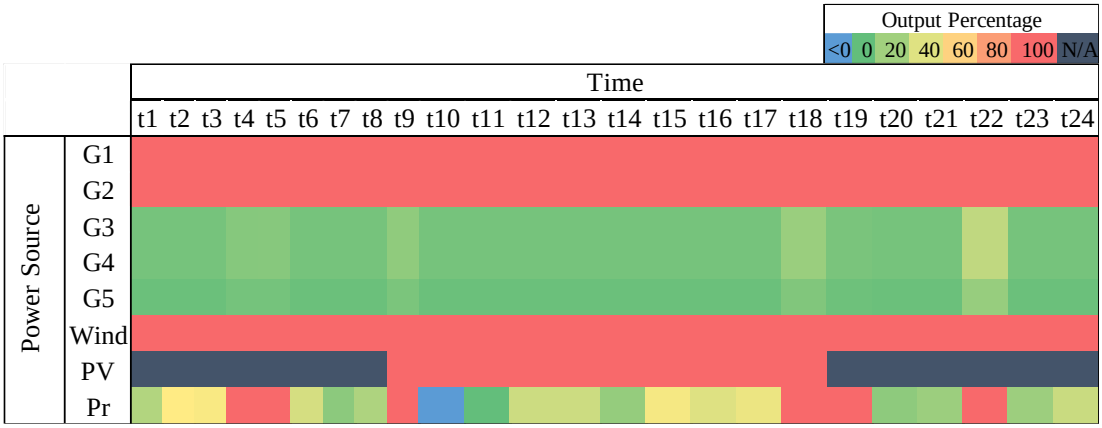

Figure 5 Percentage Output of The Generation Sources: Case One-Final Case

The N/A cells (grey color) refer to the cases when a generation source has a zero-generation capacity in a certain period, like the PV system at night. The blue color is exclusive for the transfer bus when electricity is sold to the main grid.

Analyzing the above figures shows the validity of the leader's model in trying to minimize costs:

- Clean energy: the costs of power generation from the PV and wind turbines is zero. Therefore, to minimize generation costs they have to be fully utilized throughout the day as shown in Figure 4 and Figure 5.
- Conventional generation units: their generation costs in Appendix A show that units G4 and G5 are the most expensive to operate, and units G1 and G2 are the least expensive. Hence, the operator relies mostly on G1 and G2 to supply the required load.
- Transferred power: power purchasing from the grid is mainly less expensive than utilizing G4 and G5 units at even half their generation capacities. Therefore, the transferred power varies the most among the power sources. In the final load case, in period t10, a small amount of power (-1.37kW) is generated and sold to the main grid to reduce total costs.

Market prices: The prices of the base case, first and last iterations are shown in Figure 6. These reflect the results of (16). For example, in the initial load in period t4, the output of generation unit G5 (7.95kW) results in the market price of ¢2.131/kWh $(2 \times 0.09 \times 7.95 + 0.7)$.

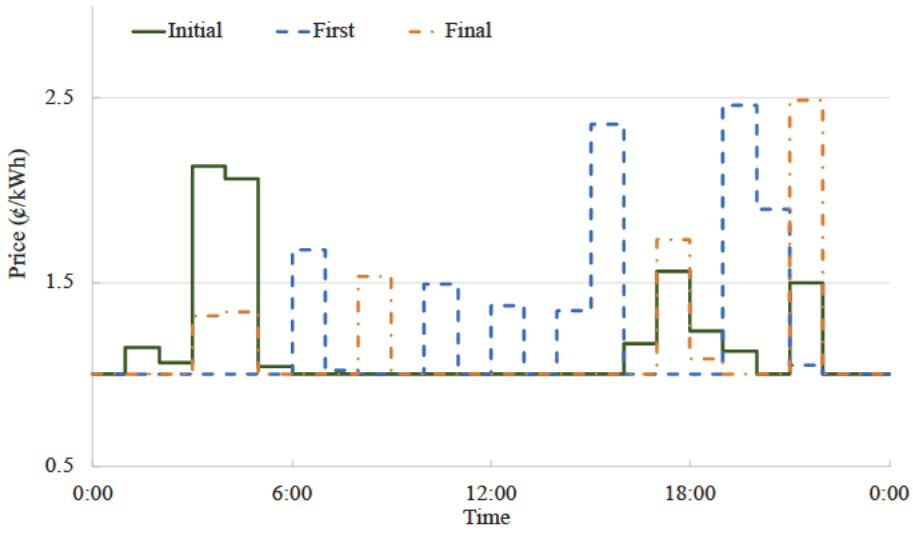

Figure 6 Market Prices in Different Iterations in Case One

Load change: The changes in the residential and the industrial load through the base case, first and last iterations are shown in Figure 7 and Figure 8 respectively. These reflect the strategies played by the followers' as a response to the market prices.

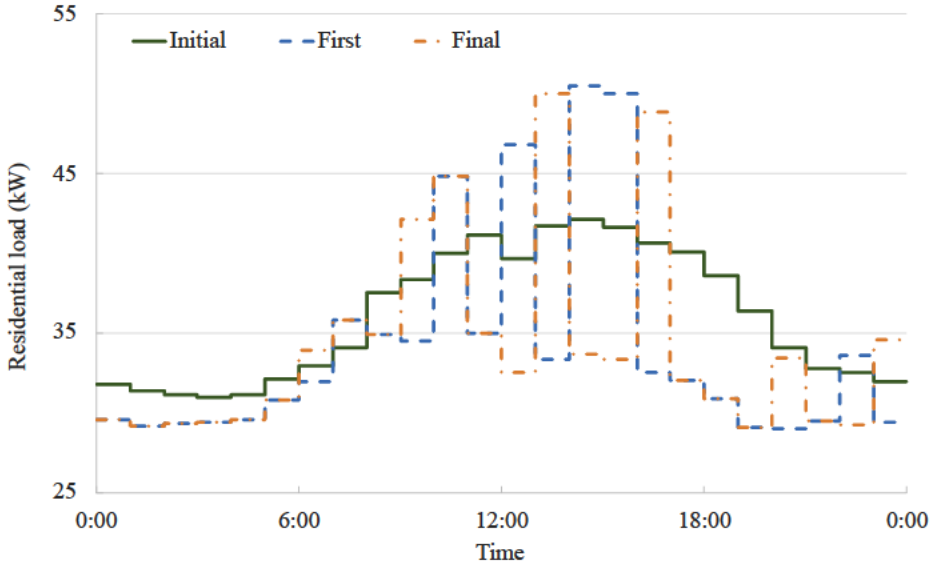

Figure 7 Daily Residential Loads in Different Iterations: Case One

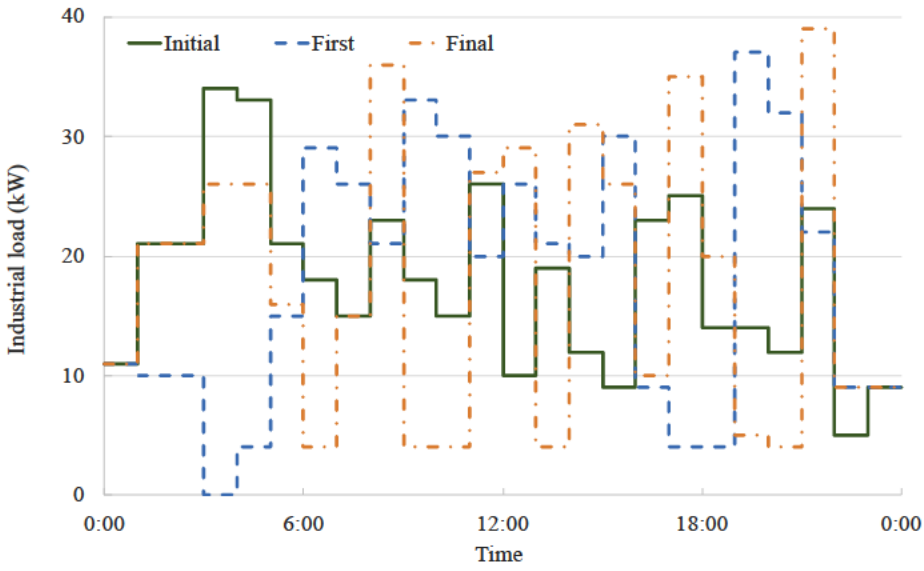

Figure 8 Daily Industrial Loads in Different Iterations: Case One

The initial prices shown in Figure 6 correspond to the economic dispatch of the initial loads in Figure 7 and Figure 8. These refer to the basic case where customers do not participate in the RTP DR program. The values of the first iteration reflect the results of economic dispatch with rigid but detailed modeling of the residential and industrial consumers after acting to the prices evaluated based on the initial load. Finally, the results of the last iteration refer to the output of the proposed model i.e. the modified

Stackelberg game approach. Here, there was no change in the load compared to the previous iteration.

Residential load: the change of the residential load is obvious as shown in Figure 7. The RTP constraint is verified where the load is lower than how it was in the initial iteration at the beginning, then surpasses it at later times. This shows how loads are not shifted to earlier times.

Industrial load: As mentioned before, the operation of a machine and equipment in the manufacturing scheme will affect the status of other machines. The goal of the industrial consumers is to profit the most and hence the machines should be scheduled optimally to reduce electric bill costs. The machines' status of the final load is shown in Table 2 and their buffer storage is shown in Table 3.

Table 2 Machines On/Off Status: Case One-Final Case

		Machine									
		r0.c1	r0.c2	r1.c1	r1.c2	r1.c3	r2.c1	r3.c1	r3.c2	r3.c3	r3.c4
Time	t1	0	0	1	0	0	0	1	0	0	0
	t2	0	0	1	1	0	0	1	1	0	0
	t3	0	0	1	1	0	0	1	1	0	0
	t4	0	0	1	1	0	0	1	1	1	0
	t5	0	0	1	1	0	0	1	1	1	0
	t6	0	0	1	1	0	0	0	1	0	0
	t7	0	0	0	1	0	0	0	0	0	0
	t8	0	0	1	1	0	0	1	0	0	0
	t9	0	0	1	1	1	1	0	1	1	1
	t10	0	0	0	1	0	0	0	0	0	0
	t11	0	0	0	1	0	0	0	0	0	0
	t12	1	0	1	1	1	0	1	0	0	1
	t13	1	0	1	1	0	1	0	1	0	0
	t14	0	0	0	1	0	0	0	0	0	0
	t15	1	0	1	1	1	1	1	0	0	0
	t16	1	0	1	1	0	0	0	1	1	0
	t17	0	0	1	1	0	0	0	0	0	0
	t18	1	0	1	1	1	1	1	0	0	1
	t19	1	0	0	1	0	0	1	1	0	0
	t20	1	0	0	0	0	0	0	0	0	0
	t21	0	0	0	1	0	0	0	0	0	0
	t22	1	1	0	1	1	1	0	1	1	1
	t23	1	1	0	0	0	0	0	0	0	0
	t24	1	1	0	0	0	0	0	0	0	0

Table 3 Number of Items in Buffers: Case Number- Final Case

		Buffer									
		r0.c1	r0.c2	r1.c1	r1.c2	r1.c3	r2.c1	r3.c1	r3.c2	r3.c3	r3.c4
Time	t1	0	0	72	0	0	0	24	0	0	0
	t2	0	0	96	12	0	0	24	12	0	0
	t3	0	0	120	24	0	0	24	24	0	0
	t4	0	0	144	36	0	0	24	12	24	0
	t5	0	0	168	48	0	0	24	0	48	0
	t6	0	0	192	60	0	0	0	12	48	0
	t7	0	0	144	72	0	0	0	12	48	0
	t8	0	0	168	84	0	0	24	12	48	0
	t9	0	0	192	48	24	72	0	0	42	30
	t10	0	0	144	60	24	72	0	0	42	30
	t11	0	0	96	72	24	72	0	0	42	30
	t12	12	0	120	36	36	36	24	0	12	48
	t13	24	0	144	48	24	72	0	12	12	36
	t14	24	0	96	60	24	72	0	12	12	36
	t15	36	0	120	24	36	108	24	12	12	24
	t16	48	0	144	36	24	72	0	0	36	12
	t17	48	0	168	48	24	72	0	0	36	12
	t18	60	0	192	12	36	108	24	0	6	30
	t19	72	0	144	24	24	72	24	12	6	18
	t20	84	0	144	24	12	36	24	12	6	6
	t21	84	0	96	36	12	36	24	12	6	6
	t22	56	40	48	0	24	72	0	0	0	24
	t23	28	80	48	0	12	36	0	0	0	12
	t24	0	120	48	0	0	0	0	0	0	0

These patterns and numbers in Table 2 and Table 3 demonstrate the validity of the industrial model:

- A machine does not operate unless the previous machine in the same manufacturing line has previously functioned.
- The buffer storage equations for non-assembly (r>0) and assembly lines (r=0) have been verified. For example:
  1) Machine r1.c1 generates $\frac{60\times60}{50} = 72$ units/hour, and the consecutive machine r1.c2 generators 12 units/hours and requires 4 units of the previous machine to manufacture 1 unit. With the buffer of r1.c1 already having 72 units at t1, and both machines turned on in t2: then the number of units in buffer r1.c2 at t2 = $72 + 72 - 4 \times 12 = 96$ as verified in Table 3.
  2) Similar analysis on the machine at the beginning of the assembly lines shows the change in the buffers at the end of the non-assembly lines.
  3) The constant increase of units of the last buffer shows how the final products are accumulated.

- The zero or minimal leftovers units in the buffers at t24 verify the optimal scheduling of units by utilizing the machines as efficiently as possible and optimally purchasing the extra materials needed by machines in the first columns.

Objective functions: The variations of the objective functions throughout the iterations are shown in Table 4.

Table 4 Iterations Output: Case One

Iterations	OF2(¢)	OF3(¢)	OF1(¢)
Initial	-	-	770.660
First	943.290	72980.588	743.036
Second	1000.86	72831.685	729.598
Third	922.456	72991.343	754.015
Fourth	1052.25	72789.226	728.392
Final	930.068	72886.228	-

5.1.3 Discussion and analysis

The optimal dispatch without considering demand response (base values) results in a total generation cost per day of ¢770.66. As observed in Figure 7, the residential load peaks in the afternoon and dips after midnight, whereas the industrial load is initially high from 3:00 till 5:00. This results in high generation costs and electricity prices during these periods.

After the first iteration, the total generation cost per day is reduced to ¢743.036. This outcome is a better optimum than the initial value since the economic dispatch now considers a more detailed representation of the loads. In addition, the 5% sheddable residential load contributes to a further decrease in OF1. Besides this cut in the total load, the residential load drops at peak prices (3:00 → 5:00) and after 17:00, when the prices are higher than previous hours. On the contrary, it spikes during 12:00 → 13:00 and 14:00 →16:00. Similarly, the industrial customers operate their machines with lower capacity at peak price hours. In fact, when the prices are at their maximum (3:00 → 4:00), the industrial load is 0. More machines operate during the day due to the lower prices, compared to the initial case. However, the demand response behavior of the consumers is still not well represented, since, with the new resulting prices, the loads are expected to change.

After the iterations converge, economic dispatch results in a total cost of ¢728.392, a 5.48% drop in cost compared to the initial values, and a 2% drop compared to the first iteration As shown in Figure 7 and Figure 8, new residential and industrial peaks emerged compared to the base case and the first iteration. By simulating the behavior of the consumers and more accurately accounting for demand response, a more optimal economic dispatch was achieved. Furthermore, the model indicates that the operator is not the only profited player in DR programs. There is a drop of 1.42% in the residential bill. The profit of the industrial load, however, decreased from iteration 1 to the last iteration. It is important to repeat that the primary optimization is from the perspective of the operator.

To further assess the impact of DR in reducing the costs, the load factor is studied. The load factor is defined as the ratio between the average demand and the peak demand in a certain period. A 100% load factor reflects a flat curve of demand, i.e. a fixed demand throughout the whole day. With DR programs, a higher load factor can be achieved with its potential in load shifting and shedding.

With the presence of zero-cost green energy sources, the operator aims to fully utilize them for minimum cost, and hence the goal is to match the load with the green DGs. Therefore, to fully understand the impact of DR in load shifting and minimizing the generation costs of the conventional units, the generation output of the PVs and the wind turbines in the systems are deducted from the total demand when measuring the load factor.

The load factor of the total demand in the initial case was 62.23% and increased to 70.10% in the final case.

5.2 Case Study 2: IEEE 24-RTS

5.2.1 Network description

In this case study, the model is tested on the IEEE 24 bus reliability test system with bus 13 being the slack bus. The model is restructured from [49] and shown in Figure 9. A non-discrete industrial load is tested to not only consider more possible scenarios

but to test the convergence of the model with more elastic and flexible loads. A discrete operation would give fewer possibilities than a non-discrete case.

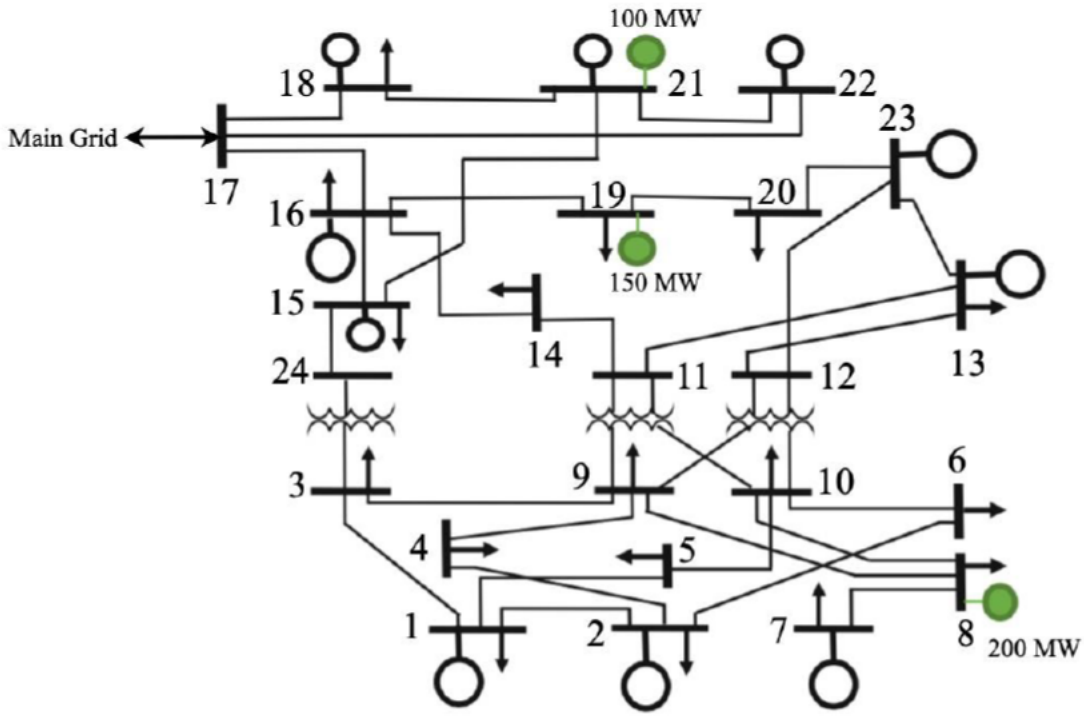

Figure 9 Updated 24 Bus RTS

The system consists of several power sources with different generation capacities and costs. In Appendix B, the technical characteristics of the network are shown. The residential load throughout the day and their shifting limits are listed in Appendix B as well.

A bigger industrial scheme is studied in this case study as shown in Figure 10. This load replaces the initial load on bus 18 in [49]. The initial statuses of the machines, their electrical demand, and other characteristics are detailed in Appendix B.

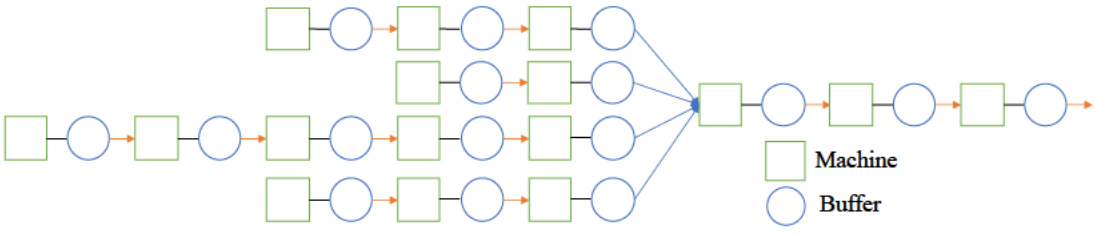

Figure 10 Industrial Load Scheme Number Two

5.2.2 Results

The GAMS model is tested on the NEOS server [50]–[52]. The bigger model took 10 iterations to converge, with the industrial load being the same as the previous iteration and the residential load having minimal changes.

Market prices: The prices of all the iterations are shown in Figure 11.

Load change: The changes in the residential and the industrial load through the iterations are shown in Figure 12 and Figure 13 respectively.

Objective functions: The variations of the objective functions through the iterations are shown in Table 5.

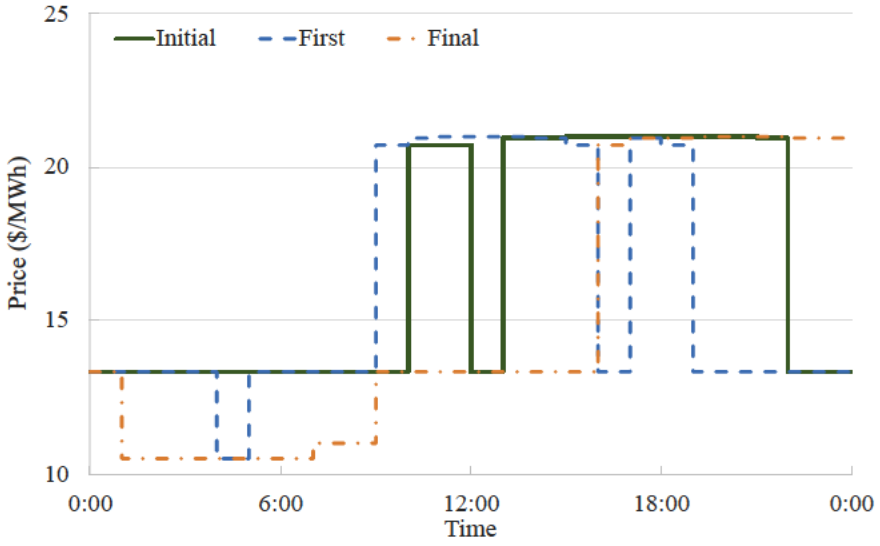

Figure 11 Market Prices in Different Iterations: Case Two

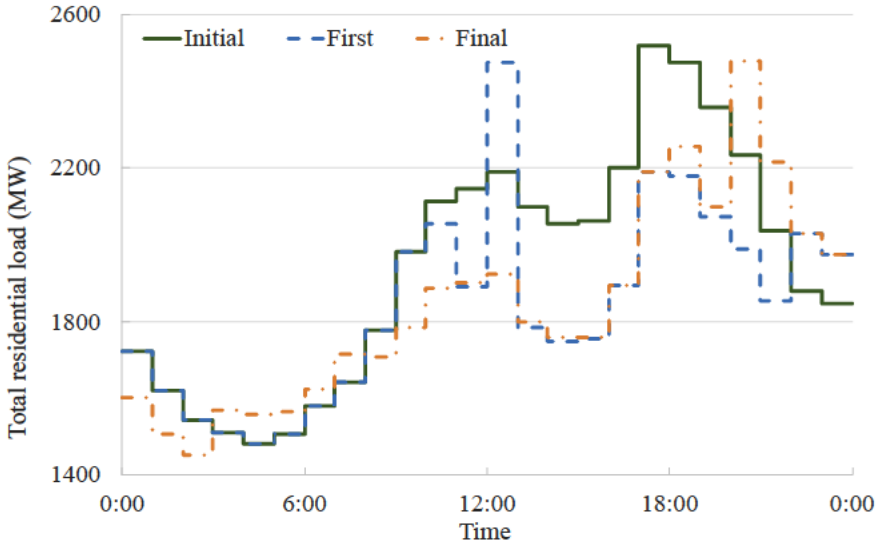

Figure 12 Daily Total Residential Loads in Different Iterations: Case Two

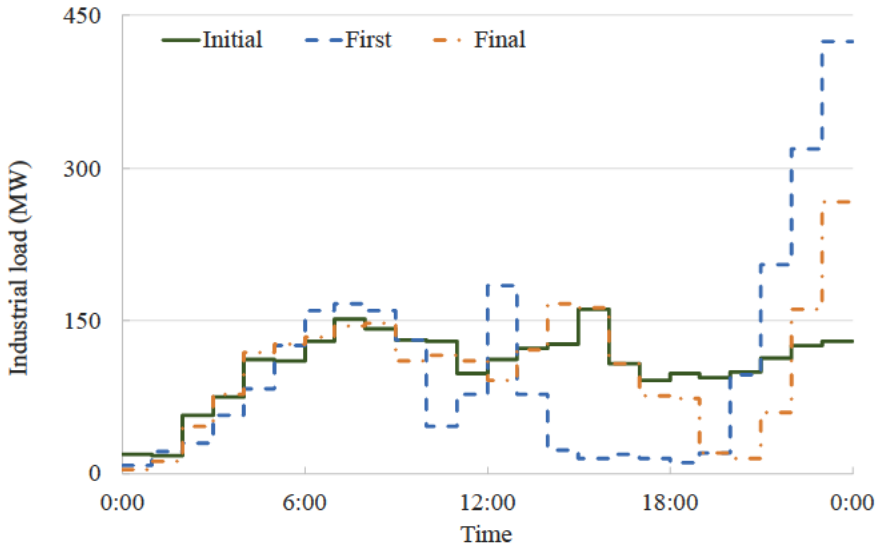

Figure 13 Daily Industrial Loads in Different Iterations: Case Two

.

Table 5 Iterations Output Case Two

	OF2 ($)	OF3 ($)	OF1($)
Initial	-	-	322816
First	848290	242601	289358
Second	758817	244259	285505
Third	715585	246617	298952
Fourth	758255	243110	290853
Fifth	734991	243007	288564
Sixth	722758	243398	288551
Seventh	727870	241792	288666
Eighth	727129	243066	288578
Ninth	722803	243398	288541
Tenth	722769	243398	-

The market interaction is the focus of this thesis. With the model being already validated in case study one, the technical results of the system are discussed and presented in Appendix C.

5.2.3 Discussion and analysis

The optimal dispatch without considering demand response (base values) results in a total generation cost per day of $322,816. As observed in Figure 12, the residential load peaks in the afternoon and dips after midnight, whereas the industrial load is initially low at midnight and has an average consumption in the rest of the day. This results in high generation costs and electricity prices from 13:00 till 22:00.

After the first iteration, the total generation cost per day is reduced to $289,358. Again, this outcome is a better optimum than the initial value since the economic dispatch now considers a more detailed representation of the loads. In addition, the 5% sheddable residential load contributes to a further decrease in OF1. Besides this cut in the total load, the residential load drops at peak prices (13:00 → 22:00) and spikes noticeably between 12:00 and 13:00 due to the lower prices there compared to close hours. Similarly, the industrial customers operate their machines with lower capacity at peak price hours and shift most of the load to late hours (after 21:00). Again, the demand response behavior of the consumers is still not well represented, since, with the new resulting prices, the loads are expected to change.

After the iterations converge, economic dispatch results in a total cost of $288,541, a 10.62% drop in cost compared to the initial values, and a 0.28% drop compared to the first iteration. Despite this minimal change in the generation cost between the first and last iteration, the change in the units scheduling and load peaks is significant. As shown in Figure 12 and Figure 13, new residential and industrial peaks emerged compared to the base case and the first iteration. By simulating the behavior of the consumers and more accurately accounting for demand response, a more optimal economic dispatch was achieved. Again, the model indicates that the operator is not the only profited player in DR programs. There is a drop of 14.8% in the residential bill. The profit of the industrial load increased insignificantly by 0.3%.

The load factor of the total demand in the initial case was 76.98% and increased to 77.99% in the final case.

5.3 Case Study 3: IEEE 123 Bus System

5.3.1 Network description

In this case study, the model is tested on the IEEE 123 bus system with bus 1 being the slack bus. The system is inspired from [53] and shown in Figure 14. A non-discrete industrial load is tested in this system as well.

The network is powered by several distributed generation (DG) sources. In addition, this microgrid has two connections to the main grid through buses 1 and 123. The

characteristics of the sources and other technical descriptions are detailed in Appendix D. The industrial load scheme is shown in Figure 10. The residential load and industrial loads characteristics are listed in Appendix D as well.

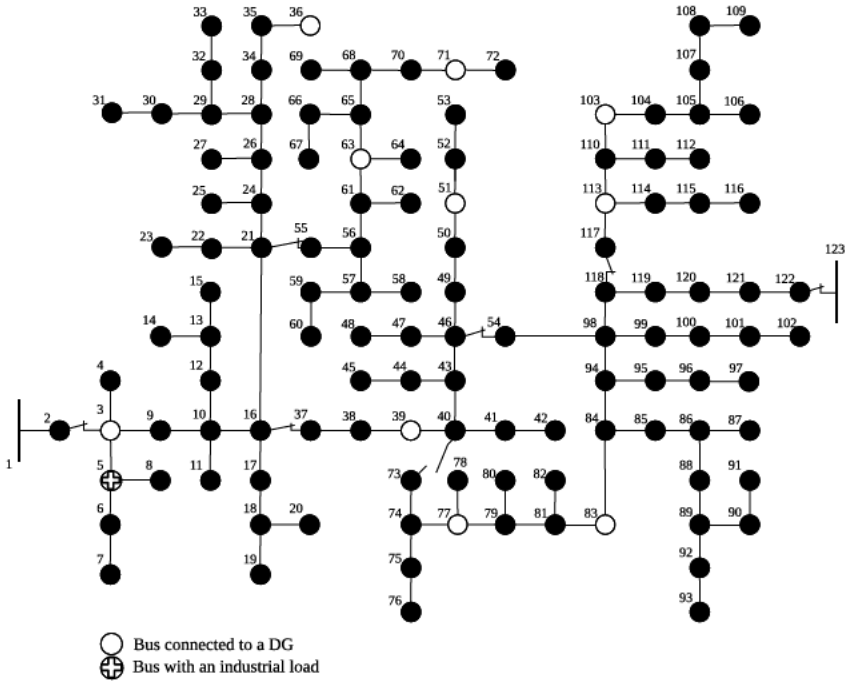

Figure 14 Modified IEEE 123-Bus System

5.3.2 Results

The GAMS model is tested on the NEOS server [50]–[52]. The model took 8 iterations for the operator to have the same prices as the previous iteration. The following data is observed:

Market prices: The prices of all the iterations are shown in Figure 15.

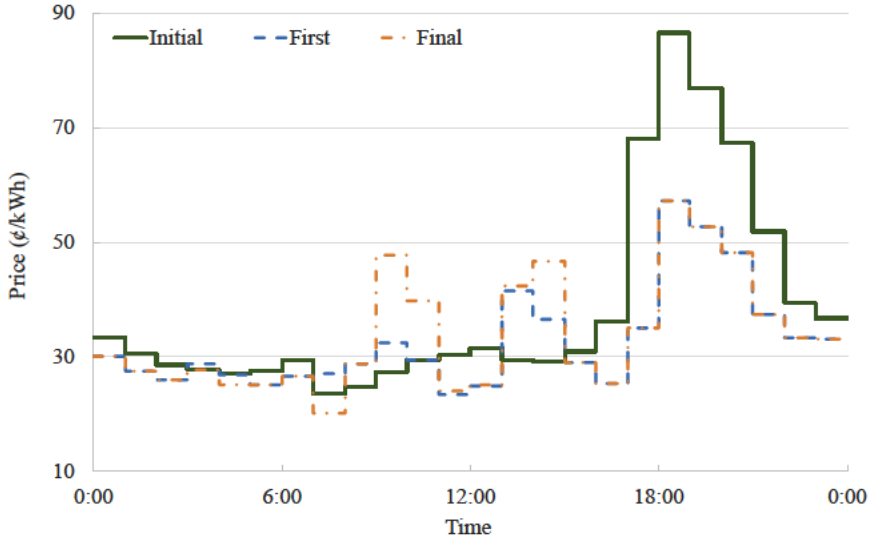

Figure 15 Market Prices Different Iterations: Case Three

Load change: The changes in the residential and the industrial load through the iterations are shown in Figure 16 and Figure 17 respectively.

Objective functions: The variations of the objective functions through the iterations are shown in Table 6.

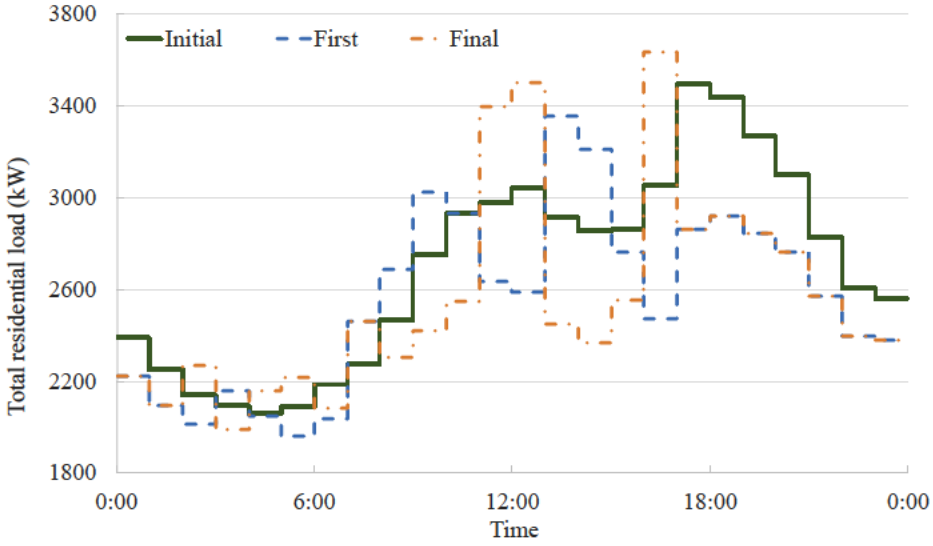

Figure 16 Daily Residential Loads in Different Iterations: Case Three

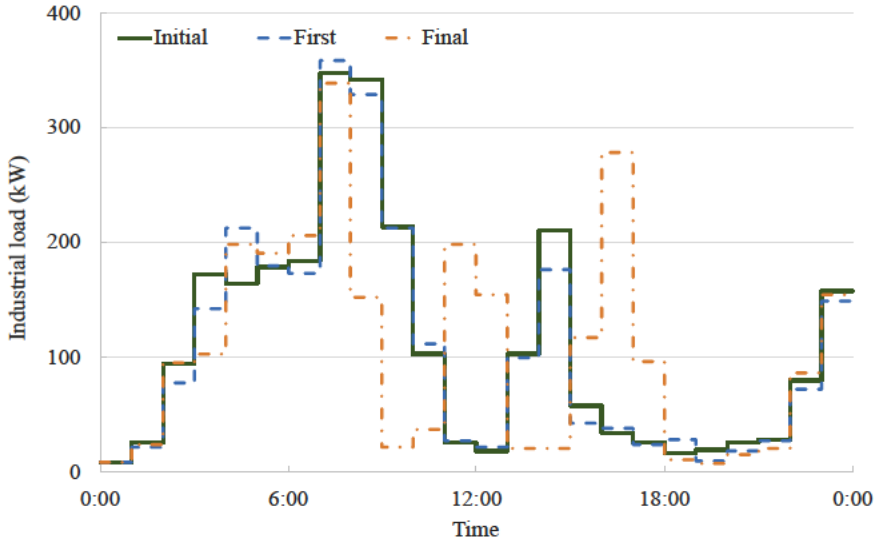

Figure 17 Daily Industrial Loads in Different Iterations: Case Three

The initial and first values displayed in Figure 15, Figure 16 and Figure 17 reflect the nature of the iterations as in the previous case studies. Similarly, the results of the last iteration refer to the output of the proposed model. However, in this case, there was an insignificant change in the prices (not loads) compared to the previous iteration. Consequently, the iterative process was terminated.

Table 6 Iterations Output: Case Three

Iterations	OF2(¢)	OF3(¢)	OF1(¢)
Initial	-	-	7154.72
First	26908.44	69759.38	6155.60
Second	21337.74	69816.41	6393.56
Third	23706.76	69854.98	6230.71
Fourth	22312.62	69834.42	6353.53
Fifth	23084.24	69852.78	6242.46
Sixth	22552.85	69831.98	6358.37
Seventh	23087.85	69856.29	6240.31
Final	22498.96	69838.46	6239.15

More technical results of the system in the final iteration of this case study is presented are Appendix E.

5.3.3 Discussion and analysis

The optimal dispatch without considering demand response (base values) results in a total generation cost per day of ¢7154.72. As observed in Figure 15, the residential load peaks in the evening and dips after midnight, whereas the industrial load is initially high between 7:00 and 9:00. The industrial load is not a significant part of the total load, therefore there are high generation costs and electricity prices in the evening.

After the first iteration, the total generation cost per day is reduced to ¢6155.60. Again, this result is a better optimum than the initial value since the economic dispatch now considers a more detailed representation of the loads and due to the 5% dip in the total residential load. As a result of the new economic dispatch, the residential loads fall significantly after 17:00, and new both residential and industrial loads peak at noon. Again, the demand response behavior of the consumers is still not well represented because customers are anticipated to optimize based on the new prices.

After the iterations converge, economic dispatch results in a total cost of ¢6239.15, a 12.8% drop in cost compared to the initial values, and a 1.36% increase compared to the first iteration. In this case study too, new residential and industrial peaks emerged

compared to the base case and the first iteration. Noticeably, the prices and loads after the hour 17:00 did not vary or scarcely altered after the initial iteration.

This model also indicates that the operator is not the only profited player in DR programs. There is a significant drop in the residential bill by 16.39%. Lastly, the profit of the industrial load barely increased by 0.11% from iteration 1 to the last iteration. As a result, the equilibrium generation cost and customers' loads can considerably differ from their base load and their first response to new RTP prices.

The load factor of the total demand in the initial case was 75.2% and increased to 79.74% in the final case.

Chapter Six

Elaborate Energy Management Model for the Industrial Consumers

6.1 Energy Storage Applications

In addition to providing ancillary services to the electricity grid [54],[55]. and supporting renewable-energy-based island grids [56],[57], electricity storage can play an important role in customer energy management systems [58]. In [59], the authors propose an algorithm that schedules the use of electricity storage and heating, ventilation, and air conditioning (HVAC) systems of buildings to minimize their costs. They show that co-optimizing the two systems together results in a significant decrease in energy costs. In [60], Rainfall Counting Algorithm and Particle Swarm Optimization techniques are used to model the behavior of thermal and electrochemical storage systems and to minimize day-ahead operation costs for residential loads. Using peer-to-peer energy trading between residential consumers, with energy storage, to coordinate DR schemes is proposed in [61]. The authors present a model that optimally schedules household equipment and energy storage under day-ahead or hour-ahead intraday markets as well as an optimal bidding strategy for these households. In [62], the importance of energy storage for residential prosumers with PV systems is discussed. Electrical load and available PV power are forecasted using deep learning neural network algorithms for optimal scheduling of demand in a day-ahead, time-of-use pricing market. Additionally, a rule-based controller is suggested to reduce losses, due to errors in forecasting, in real-time.

6.2 Related Work

Energy management of industrial facilities with discrete manufacturing models and energy storage is studied in [63] and [64]. In [63], the authors formulate an optimal load dispatch problem of industrial consumers, with Distributed Energy Resources

(DERs) and energy storage, in response to RTP. Their objective is to minimize the cost of these consumers, including fuel, DER maintenance, and electricity purchasing cost while meeting a given target for product manufacturing. In [64], a model that determines the load reduction capability of industrial consumers in response to incentive-based DR is presented. The model minimizes the completion time of the manufacturing process for a given set of product orders while reducing electricity purchasing costs and considering electricity storage and PV production. In both papers, the authors consider a fixed manufacturing output and a pre-determined electricity storage capacity.

The objectives of the elaborate model are: 1) to present a model that optimizes the energy management and product output of an industrial facility with discrete manufacturing processes and electricity storage, 2) to propose an approach for the optimal sizing of the electricity storage used by these facilities, and 3) to illustrate the role that electricity storage can play in maximizing their profits.

6.3 Energy Management Model with ESS

6.3.1 Objective function

The objective of the industrial consumer is similar to the one considered in Chapter Four but with the additional consideration of energy storage. Moreover, the elaborate model further includes labor costs and the minimal power consumption of the machines when they are turned off. The objective function in the elaborate model *OF4* is shown in (35).

$$\max OF4 = B_{0M_0t_{24}}(Ks - l) - \sum_{t=1}^{T}\sum_{r=1}^{S} KP_r\beta_r n_{r1t} - \sum_{t=1}^{T} Price_t E_t \qquad (35)$$

Where l is the labor cost of production per item and E_t is the power needed by the industrial facility from the grid.

6.3.2 Constraints

The industrial operation constraints are the same as in (23) → (30). The added energy storage constraints are as follows:

The State of Charge in a period t of the ESS (SoC_t) equals the state of charge in the previous period plus the charge added (Ec_t) minus the charge used (Ed_t) as illustrated in (36).

$$\mathrm{SoC}_t = \mathrm{SoC}_{t-1} + \mathrm{Ec}_t - \mathrm{Ed}_t \quad , t \in T \tag{36}$$

The ESS has upper storage capacity ($\overline{\mathrm{SoC}}$) and naturally cannot be negative.

$$0 \leq \mathrm{SoC}_t \leq \overline{\mathrm{SoC}} \quad , t \in T \tag{37}$$

The ESS cannot instantly charge or discharge. These limits ($\overline{\mathrm{Ec}}$ and $\overline{\mathrm{Ed}}$) are shown in (38) and (39).

$$0 \leq \mathrm{Ec}_t \leq \overline{\mathrm{Ec}} \times xc_t \quad , t \in T \tag{38}$$

$$0 \leq \mathrm{Ed}_t \leq \overline{\mathrm{Ed}} \times xd_t \quad , t \in T \tag{39}$$

Where xc_t and xd_t are binary variables to indicate the charging and discharge statuses of the ESS respectively.

The ESS is assumed not to be able to charge and discharge at the same time. Therefore, xc_t and xd_t cannot sum up to 2.

$$xc_t + xd_t \leq 1. \quad , t \in T \tag{40}$$

The energy to be charged for electrical bill E_t is shown in (41). The first part reflects the energy needed by the machines to operate. The machines are assumed to consume a small amount of energy even when they are turned off. The second part is the energy needed to charge the ESS when necessary. The charging efficiency η_C is to reflect the energy consumed to charge the ESS. The last part is the discharging part of the ESS which lowers the need for electrical power from the utility. Also, a discharging efficiency η_D is considered because not all the charged energy can be consumed.

$$E_t = \sum_{r=0}^{S} \sum_{c=1}^{M_r} (x_{rct} Eon_{rc} + (1 - x_{rct}) Eoff_{rc}) + {}^{\mathrm{Ec}_t}/_{\eta_C} - \mathrm{Ed}_t \cdot \eta_D \quad , t \in T \tag{41}$$

In a period t, the discharged power by the ESS cannot exceed the power needed by the industrial load.

$$\mathrm{Ed}_t \cdot \eta_D \leq \sum_{r=0}^{S} \sum_{c=1}^{M_r} (x_{rct} \times Eon_{rc} + (1 - x_{rct}) \times Eoff_{rc}) \quad , t \in T \tag{42}$$

Finally, the industrial facility is assumed to not be capable of selling electricity to the grid. Therefore, the power consumed cannot be negative.

$$0 \leq E_t \quad , t \in T \tag{43}$$

6.4 Case Study 4

6.4.1 System description

In this section, a case study to verify the validity of the optimization problem proposed is carried out.

The schematic diagram of the industrial facilities is shown in Figure 18. The characteristics and the parameters of the machines are listed in Table 7.

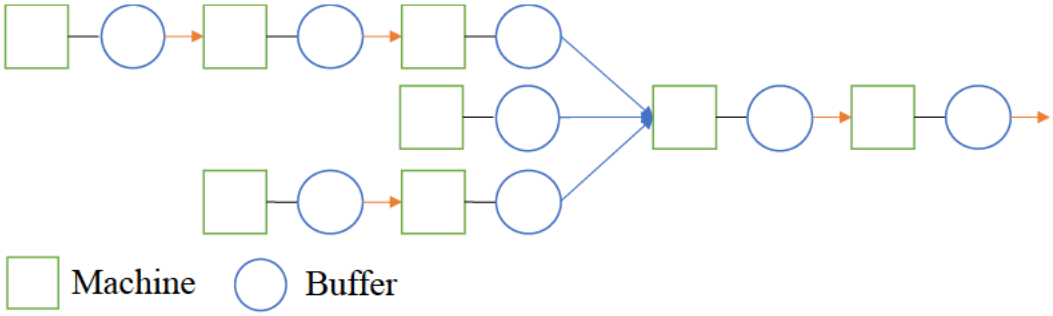

Figure 18 Schematic Diagram of Studied Industrial Load

The selling price of the product is Ks = €9.30. The labor cost of each product is l = €1.20. All the machines are assumed to consume $Eoff_{rc}$ = 0.5kW when turned off. The day studied is divided into 24 hours (Ts = 3600s). The day-ahead hourly prices ($Price_t$) are displayed in Table 8.

Table 7 Industrial Facility Parameters

Machine	CT_{rc}(s)	CAP_{rc}	Eon_{rc}(kW)	α_{rc}	KP_r(cents)	β_r
r1.c1	50	350	65	3	20	3
r1.c2	300	55	43	1	-	-
r1.c3	300	55	31	2	-	-
r2.c1	50	350	65	3	20	3
r3.c1	60	120	81	2	20	3
r3.c2	90	80	65	1	-	-
r0.c1	300	50	65	1	-	-
r0.c2	360	2000	74	-	-	-

The ESS has an upper storage capacity of $\overline{SoC}$ = 500kWh. The charge and discharge rate in a period are assumed to be 30% of the maximum capacity: $\overline{Ec}$ = $\overline{Ed}$ = 150kWh. The charging efficiency is η_C = 95% and the discharging efficiency is η_D = 80%.

Table 8 Day-Ahead Prices

Hours	$Price_t$ (€/MWh)	Hours	$Price_t$ (€/MWh)
0:00 - 1:00	10.76	12:00 - 13:00	41.87
1:00 - 2:00	5.01	13:00 - 14:00	29.75
2:00 - 3:00	4.04	14:00 - 15:00	25.01
3:00 - 4:00	3.77	15:00 - 16:00	18.02
4:00 - 5:00	4.19	16:00 - 17:00	18.02
5:00 - 6:00	14.7	17:00 - 18:00	22.07
6:00 - 7:00	23.91	18:00 - 19:00	36.33
7:00 - 8:00	39.98	19:00 - 20:00	36.54
8:00 - 9:00	41.99	20:00 - 21:00	33.93
9:00 - 10:00	42.44	21:00 - 22:00	35.25
10:00 - 11:00	42.23	22:00 - 23:00	34.25
11:00 - 12:00	41.31	23:00 - 0:00	19.7

6.4.2 Results

Two scenarios were studied: 1) industrial facility without electricity storage (w/o ESS), 2) industrial facility with electricity storage (w/ ESS). The optimization problems are thus solved by maximizing (35) subject to (23)→(30),(36)→(43) using mixed-integer programming. The SCIP solver on GAMS was utilized for solving the models.

Profit: The profit of the industrial facility without an ESS was OF4 = €88.43073, compared to OF4 = €103.43589 for the facility with ESS. A 16.968% of profit increase in one day is observed. Noticeably, with and without an ESS the industrial facility manufactured 120 products, however, with efficient energy storage and management a higher profit was achieved.

Electricity demand: The 24-hour demand for electricity from the grid is shown in Figure 19. The prices are at their maximum from 7:00 till 13:00 and are relatively high from 18:00 till 23:00. The response of the industrial facility to RTP is evident by the significantly lower demand during these high price periods compared to the rest of the day.

Energy storage: Figure 20 shows the state of charge of the electricity storage unit, as well as the charging and discharging at every hour. As expected, electricity charging occurs in periods of low energy prices, and discharging occurs in periods of high energy prices. This figure also explains the differences in the electricity demand between the two scenarios highlighted in Figure 19 and confirms the increased

flexibility provided by the electricity storage. Despite the negligible demand from 9:00 till 10:00, the industrial facility still operates powered by the ESS.

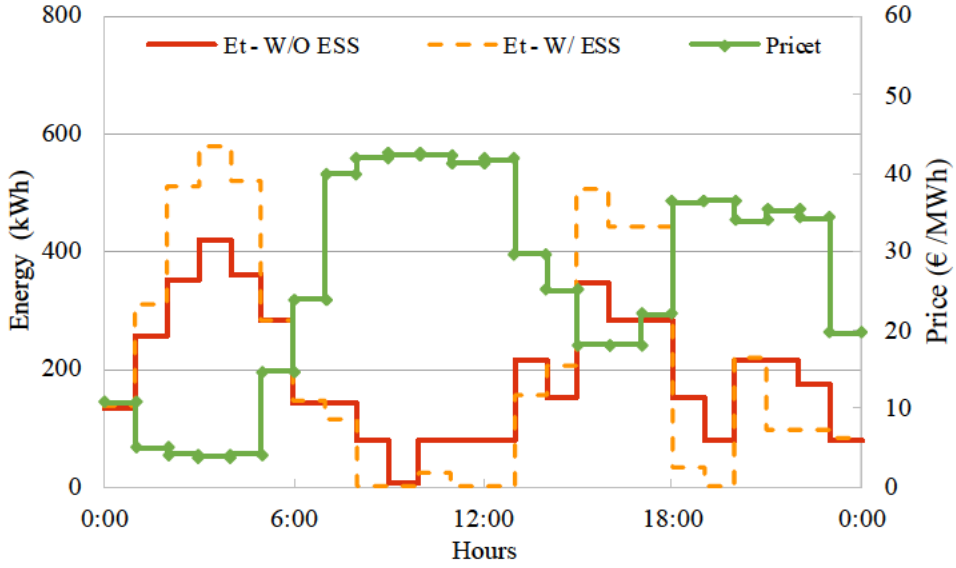

Figure 19 Energy Demand and Energy Storage at Different Hours

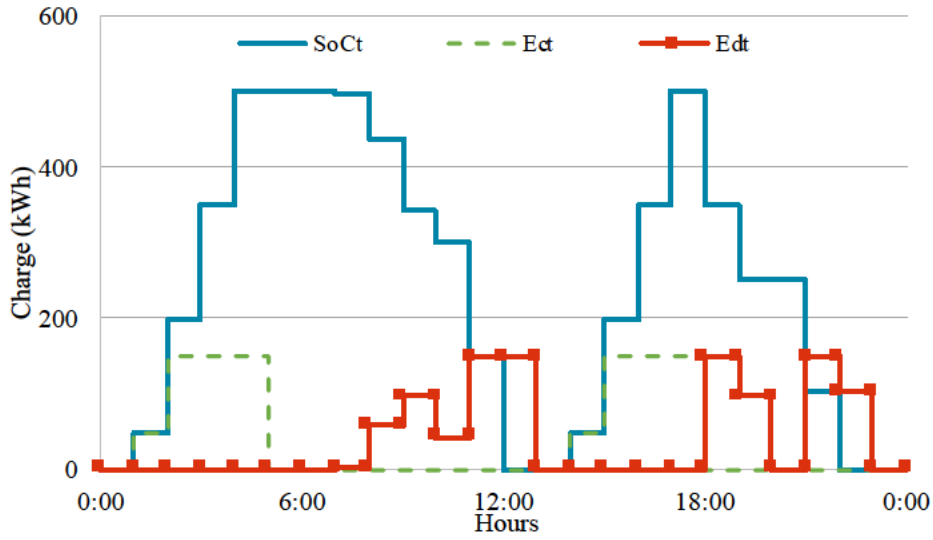

Figure 20 Charging and Discharging of the ESS System

6.5 Energy Storage Sizing Model

This section provides a model for the sizing of the ESS under day-ahead real-time pricing. In this case, the upper storage capacity of the ESS ($\overline{SoC}$) is now a variable to be determined.

The objective of the industrial facility is also to maximize the profit but with an additional cost of the installation of the ESS. Furthermore, the day-ahead prices are stochastic variables since prices are not fixed in such markets. Therefore, the number

of manufactured products and the power needed from the grid are stochastic as well. The new objective function (*OF5*) is given as:

$$\max OF5 = \mathbb{E}(\widetilde{B_{0M_0t_{24}}}(Ks-l) - \sum_{t=1}^{T}\sum_{r=1}^{S} KP_r\beta_r\widetilde{n_{r1t}} - \sum_{t=1}^{T}\widetilde{Price_t}\widetilde{E_t}) - \kappa \cdot \overline{\mathrm{SoC}} \quad (44)$$

The first four terms follow the objective function in (35), but due to the stochastic nature of some variables ($\widetilde{B_{0M_0t_{24}}}, \widetilde{n_{r1t}}, \widetilde{Price_t}, \widetilde{E_t}$) the expected value is computed. The fourth term is the installation price of the ESS, where κ is the equivalent cost of installation for one day in cents/kWh.

In [65], the authors transformed the stochastic variables into a probability density function (PDF). In the proposed model, daily *k* scenarios are considered each with a probability φ^k. The PDF of these scenarios is thus obtained, and the new objective function can now be written as:

$$\max OF5 = \sum_{k=1}^{K}\varphi^k({B_{0M_0t_{24}}}^k(Ks-l) - \sum_{t=1}^{T}\sum_{r=1}^{S} KP_r\beta_r {n_{r1t}}^k - \sum_{t=1}^{T}({Price_t}^k {E_t}^k)) - \kappa \cdot \overline{SoC} \quad (45)$$

The nature of the discrete manufacturing process with ESS requires finding optimal integer variables. With the added decision variable for sizing ($\overline{SoC}$) the computational burden of solving such an optimization model becomes high. Therefore, considering too many scenarios becomes nearly impossible even with state-of-the-art solvers and powerful computer hardware. In addition, with unbounded limits on the value of $\overline{SoC}$, solvers will take even more considerable duration to come up with the optimal solution.

The following approach is proposed to facilitate the optimization burden:

1) reduce the number of scenarios *k* by finding the PDF of the hourly prices of comparable days.

2) find the optimal energy storage $\overline{SoC}$ for each of the new scenarios alone with the objective function separately.

$$\max OF5 = B_{0M_0t_{24}}(Ks - l) - \sum_{t=1}^{T}\sum_{r=1}^{S} KP_r\beta_r n_{r1t} - \sum_{m=1}^{M}\sum_{t=1}^{T} {\rho_t}^m \cdot E_t \cdot {Price_t}^m - \kappa \cdot \overline{SoC} \quad (46)$$

For every period *t*, the total probability of the market prices should add to one.

$$\sum_{m=1}^{M} {\rho_t}^m = 1 \quad , t \in T \quad (47)$$

3) get the maximum and the minimum of the found $\overline{SoC}$, and use them as upper and lower limits on the ESS capacity.
4) solve the new optimization problem with the fewer scenarios and the new capacity constraint.

The intent behind the proposed approach is to keep the diversity of the scenarios but with less quantity and to limit the search space and the set of solutions within a predefined interval based on optimal values of separate scenarios.

The constraints of the optimization problem remain the same as 6.3.2, however, with the additional dimension considering the set of scenarios K. Additionally, $\overline{Ec}$ and $\overline{Ed}$ are set as a percentage of $\overline{SoC}$.

6.6 Case Study 5

6.6.1 System description and results

The industrial facility studied in Case Study 4 is utilized in this case study as well. The charging and discharging limits are set as: $\overline{\mathrm{Ec}} = \overline{\mathrm{Ed}} = 0.3 \times \overline{\mathrm{SoC}}$. In this case study $\kappa = 0.01$ cents/kWh.

To obtain the PDF of the day-ahead market prices at each hour, the prices in the year 2020 in Finland were utilized [66]. This yields to $k = 366$ different sets of data. For the purposes of this study, from the data, 12 scenarios were extracted, based on a monthly division. Each scenario has a probability φ^k = (number of days/366).

For example, January is now scenario *k1* with M = 31 days, and φ^k = 0.0847. Afterward, for each scenario, the PDF of the market prices for every hour, throughout the 24-hour period of study ${\rho_t}^m$ is obtained.

The expected prices of a sample of four scenarios are shown in Figure 21.

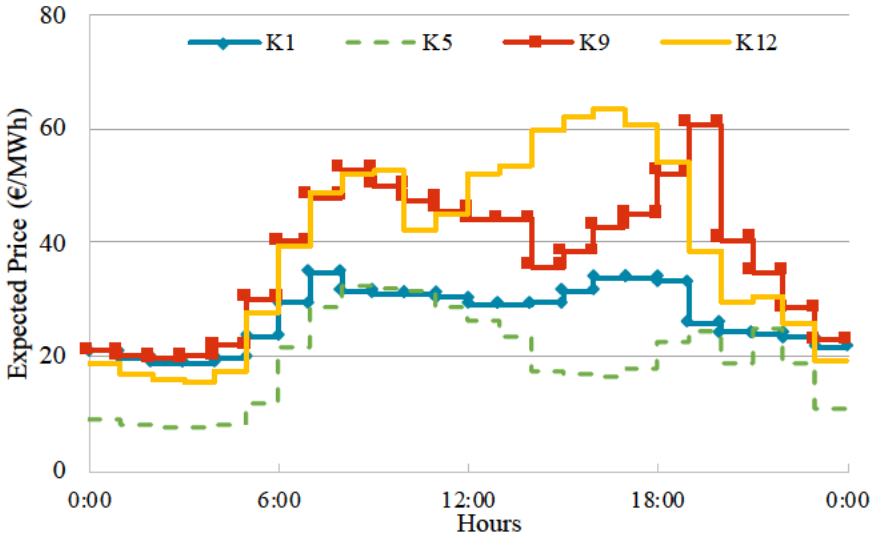

Figure 21 Expected Prices for Four New Scenarios

The different dips and peaks of the prices shown in Figure 21 in terms of occurrences and magnitude signify the alterations in the market prices that can occur in each scenario (month).

To get the upper and lower bound on $\overline{\text{SoC}}$, 12 optimization problems are solved by maximizing (46) subject to subject to (23)→(30),(36)→(43). The results obtained are shown in Table 9.

Table 9 Upper Storage Capacity for Every Scenario

Scenario k	$\overline{\text{SoC}}$ (kWh)
1	2183.75
2	3231.875
3	3500.625
4	4129.167
5	3716.25
6	3848.611
7	3813.125
8	3716.25
9	3716.25
10	3500.625
11	3813.125
12	3716.25

To obtain the upper storage capacity considering all the scenarios, (45) is maximized subject to (23)→(30),(36)→(43) with the scenario dimension. From Table 9 the additional maximum and minimum constraints, shown in (48), are added.

$$2183.750 \leq \overline{SoC} \leq 4129.167 \tag{48}$$

All the optimization models are tested on GAMS with the SCIP solver using mixed-integer non-linear programming.

The simulation results in an optimal storage capacity of 4129.167kWh and a daily expected profit of OF5 = €108.84841.

6.6.2 Sensitivity analysis

Sensitivity analysis is carried out for different values of κ to study the impact of installation costs on the sizing. The simulation results are illustrated in Table 10.

Table 10 Profit and Optimal Storage Capacity for Different ESS Installation Prices

κ (cents/kWh)	OF5 (€)	$\overline{SoC}$ (kWh)
0.005	111.54298	6193.75
0.01	108.84841	4129.167
0.05	107.31698	3366.875
0.1	105.2605	2974.375
0.3	69.9986	0

The case study results illustrate the significance of energy storage and the importance of low ESS costs in increasing profit.

At low installation costs κ = 0.005cents/kWh the profit was OF5 = €111.54298 with a high optimal storage capacity of 6193.75kWh.

With higher installation prices κ = 0.05 cents/kWh, a lower optimal energy storage capacity becomes needed ($\overline{SoC}$ = 3366.875kWh) and lower profit becomes attainable (OF5= €107.31698).

If the installation prices become high enough, the ESS will no longer make economic sense and therefore the industrial facility is better off without it as in the case when κ = 0.3 cents/kWh. The profit in such cases would be the least with OF5 = €69.9986.

6.6.3 Impact of considering several scenarios

To illustrate the importance of the proposed approach of extracting multiple scenarios, a direct comparison is made with the results of taking the entire year as a

single scenario, i.e. having a single probability distribution for each hour in the 24-hour study period.

With M = 366 days and $\kappa = 0.01$ cents/kWh, the optimization model yielded an optimal storage size of $\overline{SoC}$ = 6193.750 kWh which highly differs from the solution obtained when considering 12 scenarios. Calculating profit of the facility with this storage size but based on the 12 scenarios, results in OF5 = €97.96336, a 10% drop from the value calculated in the previous subsection. It is interesting to note that 6193.750 kWh was outside the range of values considered in the case with 12 scenarios.

Chapter Seven

Conclusion

This work presented a new model to help the network operator better predict the loads that will occur under a real-time pricing demand response program. The model combined an iterative form of the Stackelberg game technique and classic optimization methods to come up with the optimal strategies for the operator, the residential consumers, and industrial consumers.

The game model considered is the Stackelberg game where the dominant player or the leader is the operator who sets the market price, and the followers are the consumers who only know the prices in the market. The Stackelberg model considers that customers cannot collectively decide on their new consumption patterns to further enhance their benefit from DR programs, but a more realistic case where the decision is taken on an individual level. In addition, the operator tries to predict the new loads under RTP, hence he/she simulates the behavior of the customers. Therefore, the model is applied only in microgrids where the customers' objectives, constraints, and parameters could be better retrieved.

To find the optimal strategies of the players, classic optimization techniques are used. The model detailed the customers' constraints depending on the nature of their consumption. It also considered the network's physical constraints and other generation limitations for the operator that could highly affect the generation costs. The optimization problem solutions can be obtained by using off-the-shelf solvers to further simplify the model.

The model is tested on three different networks, where significant differences between the initial loads, first response to real-time prices, and the final loads are shown. This confirms the advantage of the proposed model that gives the network operator to anticipate new peaks and load shifts to help maintain the reliability of the network.

Moreover, a detailed model of an industrial facility's energy management in response to real-time pricing and considering energy storage was presented. It was shown that energy storage increases the flexibility of industrial demand response, resulting in lower electricity purchasing costs and thus greater profits. Furthermore, an energy storage sizing approach was presented. The approach relies on stochastic modeling of energy prices based on historical data. A detailed case study based on a generic industrial consumer with discrete manufacturing lines was presented. It was shown that the proposed approach resulted in a more optimal sizing of energy storage. Furthermore, a sensitivity analysis was carried out to show the impact of the cost of installation of energy storage on its feasibility.

These models can be further extended to study different energy markets like time-of-use pricing, demand-side bidding, and incentive-based programs. Additionally, machine learning could be further utilized to extract scenarios from the historical data. Price prediction algorithms can also be used to enhance the PDFs of the scenarios for sizing ESS.

References

[1] Key World Energy Statistics 2020 – Analysis - IEA, IEA. [Online]. Available: https://www.iea.org/reports/key-world-energy-statistics-2020

[2] No power problem for Olympics, gov't stresses after report on July 12 blackout released. [Online]. Available: https://web.archive.org/web/20130430161257/http:/www.greekembassy.org/Embassy/content/en/Article.aspx?office=3&folder=200&article=13848

[3] A Guide to the 2011 Texas Blackouts, State Impact Texas. [Online]. Available: https://stateimpact.npr.org/texas/tag/2011-blackouts/

[4] Blackout of November 2006: important lessons to be drawn, European Commission - European Commission. [Online]. Available: https://ec.europa.eu/commission/presscorner/detail/en/IP_07_110

[5] E. van der Vleuten and V. Lagendijk, "Transnational infrastructure vulnerability: The historical shaping of the 2006 European "Blackout"," *Energy Policy*, vol. 38, (4), pp. 2042-2052, 2010.

[6] S. E. Burke, "Enemy Number One for the Electric Grid: Mother Nature," *The SAIS Review of International Affairs*, vol. 35, (1), pp. 73-86, 2015.

[7] M. A. Ponce-Jara et al, "Smart Grid: Assessment of the past and present in developed and developing countries," *Energy Strategy Reviews*, vol. 18, pp. 38-52, 2017.

[8] R. Deng et al, "A Survey on Demand Response in Smart Grids: Mathematical Models and Approaches," *IEEE Transactions on Industrial Informatics*, vol. 11, (3), pp. 570-582, 2015.

[9] A. R. Jordehi, "Optimisation of demand response in electric power systems, a review," *Renewable & Sustainable Energy Reviews*, vol. 103, pp. 308-319, 2019, DOI: 10.1016/j.rser.2018.12.054

[10] Common Demand Response Practices and Program Designs, Michigan.gov. [Online]. Available: https://www.michigan.gov/documents/energy/Common_Practices_Feb22_522983_7.pdf

[11] 2019 Assessment of Demand Response and Advanced Metering, ferc.gov. [Online]. Available: https://www.ferc.gov/sites/default/files/2020-04/DR-AM-Report2019_2.pdf

[12] Capacity Bidding Program, Sce.com. [Online]. Available: https://www.sce.com/sites/default/files/inline-files/CBP%2BFact%2BSheet%2B0117_WCAG_K_1485979418%20%281%29.pdf

[13] The Capacity Bidding Program California, CPower Energy Management. [Online]. Available: https://cpowerenergymanagement.com/capacity-bidding-program/

[14] Capacity Bidding Program, Pge.com. [Online]. Available: https://www.pge.com/en_US/large-business/save-energy-and-money/energy-management-programs/energy-incentives/third-party-programs-capacity-bidding.page

[15] Time-Of-Use Tariffs Innovation Landscape Brief, Irena.org. [Online]. Available: https://www.irena.org/-/media/Files/IRENA/Agency/Publication/2019/Feb/IRENA_Innovation_ToU_tariffs_2019.pdf?la=en&hash=36658ADA8AA98677888DB2C184D1EE6A048C7470

[16] Z. Hu et al, "Review of dynamic pricing programs in the U.S. and Europe: Status quo and policy recommendations," *Renewable & Sustainable Energy Reviews*, vol. 42, pp. 743-751, 2015.

[17] Kopsakangas-Savolainen, M., Svento, R. (2014). Modern energy markets: Real-time pricing, renewable resources and efficient distribution. Springer. DOI: 10.1007/978-1-4471-2972-1.

[18] Q. Xu, Y. Ding, Q. Yan, A. Zheng and P. Du, "Day-Ahead Load Peak Shedding/Shifting Scheme Based on Potential Load Values Utilization: Theory and Practice of Policy-Driven Demand Response in China," *IEEE Access*, vol. 5, pp. 22892-22901, 2017, DOI: 10.1109/ACCESS.2017.2763678.

[19] E. S. Parizy, H. R. Bahrami and S. Choi, "A Low Complexity and Secure Demand Response Technique for Peak Load Reduction," *IEEE Transactions on Smart Grid*, vol. 10, no. 3, pp. 3259-3268, May 2019, DOI: 10.1109/TSG.2018.2822729.

[20] N. Ul Hassan, Y. I. Khalid, C. Yuen and W. Tushar, "Customer Engagement Plans for Peak Load Reduction in Residential Smart Grids," *IEEE Transactions on Smart Grid*, vol. 6, no. 6, pp. 3029-3041, Nov. 2015, DOI: 10.1109/TSG.2015.2404433.

[21] D. Li, H. Sun and W. Chiu, "Achieving Low Carbon Emission Using Smart Grid Technologies," 2017 IEEE 85th Vehicular Technology Conference (VTC Spring), Sydney, NSW, 2017, pp. 1-5, DOI: 10.1109/VTCSpring.2017.8108624.

[22] X. Ai, X. Liu, W. Qiu and Y. Wang, "Bid-scheduling of demand side reserve based on demand response considering carbon emission trading in smart grid," 2010 5th International Conference on Critical Infrastructure (CRIS), Beijing, 2010, pp. 1-6, DOI: 10.1109/CRIS.2010.5617534.

[23] S. H. Madaeni and R. Sioshansi, "Using Demand Response to Improve the Emission Benefits of Wind," *IEEE Transactions on Power Systems*, vol. 28, no. 2, pp. 1385-1394, May 2013, DOI: 10.1109/TPWRS.2012.2214066.

[24] A. Chiş, J. Rajasekharan, J. Lundén and V. Koivunen, "Demand response for renewable energy integration and load balancing in smart grid communities," 2016 24th European Signal Processing Conference (EUSIPCO), Budapest, 2016, pp. 1423-1427, DOI: 10.1109/EUSIPCO.2016.7760483.

[25] A. Safdarian, M. Fotuhi-Firuzabad and M. Lehtonen, "Benefits of Demand Response on Operation of Distribution Networks: A Case Study," *IEEE Systems Journal*, vol. 10, no. 1, pp. 189-197, March 2016, DOI: 10.1109/JSYST.2013.2297792.

[26] K. Kopsidas and M. Abogaleela, "Utilizing Demand Response to Improve Network Reliability and Ageing Resilience," *IEEE Transactions on Power Systems*, vol. 34, no. 3, pp. 2216-2227, May 2019, DOI: 10.1109/TPWRS.2018.2883612.

[27] K. Kopsidas, A. Kapetanaki and V. Levi, "Optimal Demand Response Scheduling With Real-Time Thermal Ratings of Overhead Lines for Improved Network Reliability," *IEEE Transactions on Smart Grid*, vol. 8, no. 6, pp. 2813-2825, Nov. 2017, DOI: 10.1109/TSG.2016.2542922.

[28] F. S. Hillier and G. J. Lieberman, Introduction to Operations Research. (9th ed.) New York McGraw-Hill, 2010.

[29] V. K. Tumuluru, Z. Huang and D. H. K. Tsang, "Integrating Price Responsive Demand Into the Unit Commitment Problem," *IEEE Transactions on Smart Grid*, vol. 5, no. 6, pp. 2757-2765, Nov. 2014, DOI: 10.1109/TSG.2014.2331357.

[30] K. Dietrich, J. M. Latorre, L. Olmos and A. Ramos, "Demand response and its sensitivity to participation rates and elasticities," 2011 8th International Conference on the European Energy Market (EEM), Zagreb, 2011, pp. 717-716, DOI: 10.1109/EEM.2011.5953103.

[31] A. Soroudi, P. Siano and A. Keane, "Optimal DR and ESS Scheduling for Distribution Losses Payments Minimization Under Electricity Price Uncertainty," *IEEE Transactions on Smart Grid*, vol. 7, no. 1, pp. 261-272, Jan. 2016, DOI: 10.1109/TSG.2015.2453017.

[32] T. Logenthiran, D. Srinivasan and T. Z. Shun, "Demand Side Management in Smart Grid Using Heuristic Optimization," *IEEE Transactions on Smart Grid*, vol. 3, no. 3, pp. 1244-1252, Sept. 2012, DOI: 10.1109/TSG.2012.2195686.

[33] S. Hargreaves-Heap and Y. Varoufakis, Game Theory: a Critical Introduction. Oxford, England: Taylor & Francis, 2004.

[34] Z. M. Fadlullah, D. M. Quan, N. Kato and I. Stojmenovic, "GTES: An Optimized Game-Theoretic Demand-Side Management Scheme for Smart Grid," *IEEE Systems Journal*, vol. 8, no. 2, pp. 588-597, June 2014, DOI: 10.1109/JSYST.2013.2260934.

[35] P. Samadi, H. Mohsenian-Rad, R. Schober and V. W. S. Wong, "Advanced Demand Side Management for the Future Smart Grid Using Mechanism Design," *IEEE Transactions on Smart Grid*, vol. 3, no. 3, pp. 1170-1180, Sept. 2012, DOI: 10.1109/TSG.2012.2203341.

[36] P. Yang, G. Tang and A. Nehorai, "A game-theoretic approach for optimal time-of-use electricity pricing," *IEEE Transactions on Power Systems*, vol. 28, no. 2, pp. 884-892, May 2013, DOI: 10.1109/TPWRS.2012.2207134.

[37] T. Li and S. P. Sethi, “A review of dynamic Stackelberg game models,” *Discrete & Continuous Dynamical Systems - B*, vol. 22, no. 1, pp. 125–159, 2017, DOI: 10.3934/dcdsb.2017007.
[38] M. Latifi, A. Khalili, A. Rastegarnia and S. Sanei, "Fully Distributed Demand Response Using the Adaptive Diffusion–Stackelberg Algorithm," *IEEE Transactions on Industrial Informatics*, vol. 13, no. 5, pp. 2291-2301, Oct. 2017, DOI: 10.1109/TII.2017.2703132.
[39] F. Meng and X. Zeng, "A Stackelberg game-theoretic approach to optimal real-time pricing for the smart grid," *Soft Computing*, vol. 17, (12), pp. 2365-2380, 2013.
[40] Q. Zhu, P. Sauer and T. Başar, "Value of demand response in the smart grid," *2013 IEEE Power and Energy Conference at Illinois (PECI)*, Urbana, IL, USA, 2013, pp. 76-82, DOI: 10.1109/PECI.2013.6506038.
[41] M. Yu and S. H. Hong, "A Real-Time Demand-Response Algorithm for Smart Grids: A Stackelberg Game Approach," *IEEE Transactions on Smart Grid*, vol. 7, no. 2, pp. 879-888, March 2016, DOI: 10.1109/TSG.2015.2413813.
[42] F. N. Al Farsi, M. H. Albadi, N. Hosseinzadeh and A. H. Al Badi, "Economic Dispatch in power systems," *2015 IEEE 8th GCC Conference & Exhibition*, Muscat, Oman, 2015, pp. 1-6, DOI: 10.1109/IEEEGCC.2015.7060068.
[43] Y. Li and S. H. Hong, "Real-Time Demand Bidding for Energy Management in Discrete Manufacturing Facilities," *IEEE Transactions on Industrial Electronics*, vol. 64, no. 1, pp. 739-749, Jan. 2017, DOI: 10.1109/TIE.2016.2599479.
[44] M. Kumar and M. De, "Optimal load scheduling for industrial load - analysis for a generalized industrial load model," in 2019, DOI: 10.1109/ICPS48983.2019.9067735.
[45] X. Dong, X. Li and S. Cheng, "Energy Management Optimization of Microgrid Cluster Based on Multi-Agent-System and Hierarchical Stackelberg Game Theory," *IEEE Access*, vol. 8, pp. 206183-206197, 2020, DOI: 10.1109/ACCESS.2020.3037676.
[46] Y. Chen, J. Xiang and Y. Li, "SOCP Relaxations of Optimal Power Flow Problem Considering Current Margins in Radial Networks," *Energies (Basel)*, vol. 11, (11), pp. 3164, 2018.
[47] N. I. Nwulu and X. Xia, "Optimal dispatch for a microgrid incorporating renewables and demand response," *Renewable Energy*, vol. 101, pp. 16-28, 2017, DOI: 10.1016/j.renene.2016.08.026.
[48] Thenounproject.com. [Online]. Available: https://thenounproject.com
[49] A. Soroudi., “Multi-period optimal AC power flow,” in Power System Optimization Modelling in GAMS, 1st ed.: Springer International Publishing, 2017, pp. 169-173
[50] J. Czyzyk, M. P. Mesnier, and J. J. Moré, “The NEOS server,” *IEEE Comput. Sci. & Eng*., vol. 5, no. 3, pp. 68–75, 1998, DOI: 10.1109/99.714603.
[51] W. Gropp and J. J. Moré, “Optimization environments and the NEOS server,” in Approximation Theory and Optimization. Cambridge, U.K.: Cambridge Univ. Press, 1997, pp. 167–182.
[52] E. D. Dolan, R. Fourer, J. J. Moré, and T. S. Munson, The NEOS server for optimization: Version 4 and beyond Mathematics and Computer Science Division, Argonne Nat. Lab., Argonne, IL, 2002.
[53] F. Yang, X. Feng and Z. Li, "Advanced Microgrid Energy Management System for Future Sustainable and Resilient Power Grid," *IEEE Transactions on Industry Applications*, vol. 55, (6), pp. 7251-7260, 2019, DOI: 10.1109/TIA.2019.2912133.
[54] C. Opathella, A. Elkasrawy, A. A. Mohamed and B. Venkatesh, "Optimal Scheduling of Merchant-Owned Energy Storage Systems With Multiple Ancillary Services," *IEEE Open Access Journal of Power and Energy*, vol. 7, pp. 31-40, 2020, DOI: 10.1109/OAJPE.2019.2952811.
[55] J. Arteaga, H. Zareipour and N. Amjady, "Energy Storage as a Service: Optimal Pricing for Transmission Congestion Relief," *IEEE Open Access Journal of Power and Energy*, vol. 7, pp. 514-523, 2020, DOI: 10.1109/OAJPE.2020.3031526.
[56] N. L. Díaz, A. C. Luna, J. C. Vasquez and J. M. Guerrero, "Centralized Control Architecture for Coordination of Distributed Renewable Generation and Energy Storage in Islanded AC Microgrids," *IEEE Transactions on Power Electronics*, vol. 32, no. 7, pp. 5202-5213, July 2017, DOI: 10.1109/TPEL.2016.2606653.
[57] C. Sun, G. Joos and F. Bouffard, "Adaptive Coordination for Power and SoC Limiting Control of Energy Storage in an Islanded AC Microgrid With Impact Load," *IEEE Transactions on Power Delivery*, vol. 35, no. 2, pp. 580-591, April 2020, DOI: 10.1109/TPWRD.2019.2916034.
[58] F. Nadeem, S. M. S. Hussain, P. K. Tiwari, A. K. Goswami and T. S. Ustun, "Comparative Review of Energy Storage Systems, Their Roles, and Impacts on Future Power Systems," *IEEE Access*, vol. 7, pp. 4555-4585, 2019, DOI: 10.1109/ACCESS.2018.2888497.

[59] D. T. Vedullapalli, R. Hadidi and B. Schroeder, "Combined HVAC and Battery Scheduling for Demand Response in a Building," *IEEE Transactions on Industry Applications,* vol. 55, no. 6, pp. 7008-7014, Nov.-Dec. 2019, DOI: 10.1109/TIA.2019.2938481.

[60] C. A. Correa, A. Gerossier, A. Michiorri and G. Kariniotakis, "Optimal scheduling of storage devices in smart buildings including battery cycling," *2017 IEEE Manchester PowerTech,* Manchester, UK, 2017, pp. 1-6, DOI: 10.1109/PTC.2017.7981199.

[61] W. Liu, D. Qi and F. Wen, "Intraday Residential Demand Response Scheme Based on Peer-to-Peer Energy Trading," *IEEE Transactions on Industrial Informatics,* vol. 16, no. 3, pp. 1823-1835, March 2020, DOI: 10.1109/TII.2019.2929498.

[62] F. Hafiz, M. A. Awal, A. R. d. Queiroz and I. Husain, "Real-Time Stochastic Optimization of Energy Storage Management Using Deep Learning-Based Forecasts for Residential PV Applications," *IEEE Transactions on Industry Applications*, vol. 56, no. 3, pp. 2216-2226, May-June 2020, DOI: 10.1109/TIA.2020.2968534.

[63] X. Lu, K. Zhou, C. Zhang, and S. Yang, "Optimal load dispatch for industrial manufacturing process based on demand response in a smart grid," *Journal of Renewable and Sustainable Energy,* vol. 10, no. 3, p. 035503, June 2018, DOI: 10.1063/1.5023772.

[64] T. Weitzel and C. H. Glock, "Scheduling a storage-augmented discrete production facility under incentive-based demand response," *International Journal of Production Research,* vol. 57, (1), pp. 250-270, 2019, DOI: 10.1080/00207543.2018.1475764.

[65] G. Mohy-ud-din, D. H. Vu, K. M. Muttaqi and D. Sutanto, "An Integrated Energy Management Approach for the Economic Operation of Industrial Microgrids Under Uncertainty of Renewable Energy," *IEEE Transactions on Industry Applications,* vol. 56, no. 2, pp. 1062-1073, March-April 2020, DOI: 10.1109/TIA.2020.2964635.

[66] "Historical Market Data." [Online]. Available: https://www.nordpoolgroup.com/48c939/globalassets/marketdata-excel-files/elspot-prices_2020_hourly_eur.xls

Appendices

Appendix A: Simple Microgrid Network

A.1 Network's Data

The network's characteristics in the first case study are detailed in this appendix. The characteristics of the conventional generators are shown in Table 11. The lower limits of the wind and solar power are $Pw_{min} = Ps_{min} = 0$. Their upper generation capacities throughout the day are the same as in [47] and listed in Table 12. The transferrable power is limited to: $P_{r,min}$=-20kW and $P_{r,max}$=20kW and has a marginal cost of: τ = ¢1/kWh.

Table 11 Conventional Generators Data: Case One

	G1	G2	G3	G4	G5
a(¢/kW^2)	0.06	0.03	0.04	0.08	0.09
b(¢/kW)	0.5	0.25	0.3	0.6	0.7
Pmin(kW)	0	0	0	0	0
Pmax(kW)	4	6	9	20	30
Dr(kW)	3	5	8	12	20
Ur(kW)	3	5	8	12	20

Table 12 Time-Varying Parameters: Case One

Time	Pw (kW)	Ps (kW)	$P_{initial,t}$ (residential) (kW)	ϵ_t
t1	7.56	0	31.83	0.07
t2	7.5	0	31.4	0.07
t3	8.25	0	31.17	0.06
t4	8.48	0	31	0.05
t5	8.48	0	31.17	0.05
t6	9.42	0	32.1	0.04
t7	9.82	0	32.97	0.03
t8	10.35	7.99	34.1	0.05
t9	10.88	10.56	37.53	0.07
t10	11.01	13.61	38.33	0.1
t11	10.94	14.97	40.03	0.12
t12	10.68	15	41.17	0.15
t13	10.42	14.78	39.67	0.18
t14	10.15	14.59	41.7	0.2
t15	9.67	13.56	42.1	0.2
t16	8.98	11.83	41.67	0.2
t17	8.37	10.17	40.7	0.2
t18	7.61	7.66	40.07	0.2
t19	6.7	0	38.63	0.2
t20	5.72	0	36.4	0.2
t21	7.21	0	34.1	0.15
t22	7.75	0	32.8	0.1
t23	7.88	0	32.5	0.1
t24	7.69	0	32	0.08

A.2 Residential Load Data

The residential loads are equivalent to the values in [47] and the customers' shifting limits ϵ_t are shown in Table 12. 5% of the load is sheddable and 80% is non-sheddable, *i.e.*, y=5 and z=80.

A.3 Industrial Load Data

The scheme of the industrial load is the same as in Figure 2 and its characteristics are shown in Table 13. The selling price of the final product is Ks = $21.The initial status of the machines for the day are shown in Table 14.

Table 13 Industrial Load Characteristics: Case One

Machine	CT_{rc}(s)	CAP_{rc}	EOn_{rc}(kW)	α_{rc}	KP_r(¢)	β_r
r1.c1	50	300	6	4	20	6
r1.c2	300	100	4	2	0	0
r1.c3	150	100	3	1	0	0
r2.c1	50	300	8	3	30	4
r3.c1	150	300	5	2	20	3
r3.c2	300	100	6	1	0	0
r3.c3	150	100	5	1	0	0
r3.c4	120	100	4	1	0	0
r0.c1	300	500	5	1	0	0
r0.c2	90	100	4	-	0	0

Table 14 Machines Status: Case One-Initial Case

		Machine									
		r0.c1	r0.c2	r1.c1	r1.c2	r1.c3	r2.c1	r3.c1	r3.c2	r3.c3	r3.c4
Time	t1	0	0	1	0	0	0	1	0	0	0
	t2	0	0	1	1	0	0	1	1	0	0
	t3	0	0	1	1	0	0	1	1	0	0
	t4	0	0	1	1	0	1	1	1	1	0
	t5	0	0	1	1	1	0	1	1	1	1
	t6	1	0	1	1	0	0	0	1	0	0
	t7	0	0	1	1	0	1	0	0	0	0
	t8	0	0	1	1	0	0	1	0	0	0
	t9	0	0	1	1	0	1	1	0	0	0
	t10	0	0	0	1	0	1	0	1	0	0
	t11	0	0	0	1	0	0	1	1	0	0
	t12	1	0	0	1	1	1	0	1	0	0
	t13	0	0	1	1	0	0	0	0	0	0
	t14	0	0	1	1	0	0	0	0	1	1
	t15	1	0	0	1	1	0	0	0	0	0
	t16	0	0	0	1	0	0	0	0	1	0
	t17	1	0	1	1	1	0	1	0	0	0
	t18	1	1	1	1	0	0	0	1	0	0
	t19	0	0	1	1	0	0	0	0	0	1
	t20	1	0	0	1	0	0	1	0	0	0
	t21	1	0	0	1	1	0	0	0	0	0
	t22	1	1	0	0	0	0	0	1	1	1
	t23	1	0	0	0	0	0	0	0	0	0
	t24	1	1	0	0	0	0	0	0	0	0

Appendix B: IEEE 24 Bus RTS Network

B.1 Network's Data

The updated IEEE RTS 24 bus system in Figure 9 has 10 conventional or hydropower sources. Their generation capacities, generation cost, and ramping limits are shown in Table 15. The base power is 100 MVA with bus 13 being the slack bus.

Table 15 Conventional Generators Data: Case Two

Bus number	Pmax (MW)	Pmin (MW)	a ($/MW^2)	b ($/MW)	Qmax (MVA)	Qmin (MVA)	RU (MW)	RD (MW)
1	152	0	0	13.32	192	-50	21	21
2	152	0	0	13.32	192	-50	21	21
7	350	0	0	20.7	300	0	43	43
13	591	0	0	20.93	591	0	31	31
15	215	0	0	21	215	-100	31	31
16	155	0	0	10.52	155	-50	31	31
18	400	0	0	5.47	400	-50	70	70
21	400	0	0	5.47	400	-50	70	70
22	300	0	0	0	300	-60	53	53
23	360	0	0	10.52	310	-125	31	31

Three wind turbines are located on busses 8, 19, and 21. Their generation outputs throughout the day are listed in Table 16.

Table 16 Time-Varying Parameters: Case Two

Time	Wind - Bus 8 (MW)	Wind - Bus 19 (MW)	Wind - Bus 21 (MW)	ϵ_t	Ω
t1	15.73	11.80	7.87	0.07	0.68
t2	17.33	13.00	8.67	0.07	0.64
t3	23.47	17.60	11.73	0.06	0.61
t4	51.73	38.80	25.87	0.05	0.60
t5	72.27	54.20	36.13	0.05	0.59
t6	113.33	85.00	56.67	0.04	0.60
t7	130.13	97.60	65.07	0.03	0.63
t8	113.33	85.00	56.67	0.05	0.65
t9	96.80	72.60	48.40	0.07	0.71
t10	109.60	82.20	54.80	0.01	0.79
t11	151.47	113.60	75.73	0.11	0.84
t12	142.13	106.60	71.07	0.12	0.85
t13	174.13	130.60	87.07	0.13	0.87
t14	186.40	139.80	93.20	0.15	0.83
t15	193.33	145.00	96.67	0.15	0.82
t16	200.00	150.00	100.00	0.15	0.82
t17	173.87	130.40	86.93	0.14	0.87
t18	133.07	99.80	66.53	0.15	1.00
t19	131.20	98.40	65.60	0.12	0.98
t20	112.27	84.20	56.13	0.12	0.94
t21	113.07	84.80	56.53	0.11	0.89
t22	111.20	83.40	55.60	0.09	0.81
t23	144.80	108.60	72.40	0.08	0.75
t24	168.00	126.00	84.00	0.07	0.73

The power lines connecting the nodes have the impedances, charging susceptance, and capacities shown in Table 17. The sell/purchase price of transferred electricity is τ=\$11/MWh, with transferring limits of $P_{r,min}$=-300MW and$P_{r,max}$= +300MW. A 0.9 power factor is considered for the transferable power and the industrial loads.

Table 17 Line Data: Case Two

From	To	Resistance (p.u)	Reactance (p.u)	b_{sh} (p.u)	Capacity (MVA)
1	2	0.0026	0.0139	0.4611	175
1	3	0.0546	0.2112	0.0572	175
1	5	0.0218	0.0845	0.0229	175
2	4	0.0328	0.1267	0.0343	175
2	6	0.0497	0.192	0.052	175
3	9	0.0308	0.119	0.0322	175
3	24	0.0023	0.0839	0	400
4	9	0.0268	0.1037	0.0281	175
5	10	0.0228	0.0883	0.0239	175
6	10	0.0139	0.0605	2.459	175
7	8	0.0159	0.0614	0.0166	175
8	9	0.0427	0.1651	0.0447	175
8	10	0.0427	0.1651	0.0447	175
9	11	0.0023	0.0839	0	400
9	12	0.0023	0.0839	0	400
10	11	0.0023	0.0839	0	400
10	12	0.0023	0.0839	0	400
11	13	0.0061	0.0476	0.0999	500
11	14	0.0054	0.0418	0.0879	500
12	13	0.0061	0.0476	0.0999	500
12	23	0.0124	0.0966	0.203	500
13	23	0.0111	0.0865	0.1818	500
14	16	0.005	0.0389	0.0818	500
15	16	0.0022	0.0173	0.0364	500
15	21	0.00315	0.0245	0.206	1000
15	24	0.0067	0.0519	0.1091	500
16	17	0.0033	0.0259	0.0545	500
16	19	0.003	0.0231	0.0485	500
17	18	0.0018	0.0144	0.0303	500
17	22	0.0135	0.1053	0.2212	500
18	21	0.00165	0.01295	0.109	1000
19	20	0.00255	0.0198	0.1666	1000
20	23	0.0014	0.0108	0.091	1000
21	22	0.0087	0.0678	0.1424	500

B.2 Residential Load Data

The residential loads at peak on each bus are shown in Table 18. To demonstrate the load throughout the day this load is multiplied by factor Ω shown in Table 16. The shifting limits ϵ_t are shown in Table 16 as well. 5% of the load is sheddable (y=5) and 80% is non-sheddable (z = 80).

Table 18 Peak Consumption on Buses: Case Two

Bus Number	Pinitial (kW)	Qinitial (kW)
1	108	22
2	97	20
3	180	37
4	74	15
5	71	14
6	136	28
7	125	25
8	171	35
9	175	36
10	195	40
13	265	54
14	194	39
15	317	64
16	100	20
19	181	37
20	128	26

B.3 Industrial Load Data

The scheme of the industrial load is the same as in Figure 10 and its characteristics are shown in Table 19. The selling price of the final product is Ks =$45000. The ramping limit is ψ = 25%. The initial status of the machines for the day are shown in Table 20.

Table 19 Industrial Load Characteristics: Case Two

Machine	CT_{rc} (s)	CAP_{rc}	EOn_{rc} (MW)	α_{rc}	KP_r ($)	β_r
r1.c1	50	300	60	4	120	6
r1.c2	120	100	40	2	0	0
r1.c3	150	100	24	1	0	0
r2.c1	50	300	30	3	150	4
r2.c2	50	300	40	3	0	0
r3.c1	150	300	20	2	200	3
r3.c2	80	100	20	2	0	0
r3.c3	90	100	30	1	0	0
r3.c4	120	100	20	1	0	0
r3.c5	120	100	20	2	0	0
r4.c1	90	300	10	2	120	3
r4.c2	120	100	20	1	0	0
r4.c3	150	100	30	3	0	0
r0.c1	90	500	50	1	240	2
r0.c2	120	500	40	2	0	0
r0.c3	150	2000	30	-	0	0

.

Table 20 Machines Status: Case Two-Initial Case

		Machine															
		r0.c1	r0.c2	r0.c3	r1.c1	r1.c2	r1.c3	r2.c1	r2.c2	r3.c1	r3.c2	r3.c3	r3.c4	r3.c5	r4.c1	r4.c2	r4.c3
Time	t1	0	0	0	0.194	0	0	0	0	0.25	0	0	0	0	0.225	0	0
	t2	0	0	0	0	0	0	0	0	0.5	0	0	0	0	0.45	0.167	0
	t3	0	0	0	0.208	0.2	0	0.097	0	0.625	0.2	0	0	0	0.2	0.4	0.25
	t4	0	0	0	0.458	0.1	0	0	0.014	0.75	0.222	0	0	0	0.425	0.233	0.5
	t5	0	0	0	0.708	0	0	0	0	1	0.378	0.15	0	0	0.675	0.433	0.75
	t6	0	0	0	0.5	0	0	0.083	0	1	0.156	0.35	0.1	0	0.9	0.667	0.667
	t7	0	0	0	0.75	0	0.083	0	0	1	0.2	0.125	0.233	0.033	1	0.667	0.875
	t8	0.025	0	0	0.986	0	0	0.25	0.069	1	0.422	0.25	0	0.267	1	0.5	0.667
	t9	0.05	0.1	0	0.736	0.033	0.083	0.486	0.222	1	0.2	0.025	0.233	0.233	1	0.333	0.458
	t10	0.1	0	0	0.486	0.267	0.125	0.514	0	1	0.356	0.275	0	0	1	0.367	0.5
	t11	0	0	0	0.236	0.5	0.375	0.708	0.25	1	0.111	0.075	0.067	0	1	0.6	0.25
	t12	0	0	0	0	0.733	0.375	0.542	0.014	1	0.356	0	0	0.033	0.75	0.4	0
	t13	0.05	0.133	0	0	0.733	0.208	0.292	0	1	0.111	0.25	0.233	0.233	0.5	0.467	0.25
	t14	0.1	0.033	0	0.167	0.567	0	0.542	0	1	0.267	0.175	0.433	0.467	0.25	0.233	0.417
	t15	0.05	0.233	0	0.417	0.367	0.083	0.333	0.222	1	0.489	0	0.567	0.233	0	0	0.292
	t16	0.25	0	0	0.653	0.367	0.333	0.5	0.25	1	0.267	0.25	0.433	0.233	0	0	0.542
	t17	0	0	0	0.417	0.167	0.542	0.75	0	1	0.267	0	0.233	0	0.025	0	0.375
	t18	0	0	0	0.194	0	0.292	1	0	1	0.156	0.2	0.267	0	0.25	0.1	0.125
	t19	0	0	0.167	0	0.233	0.125	0.847	0.014	1	0.4	0.4	0.233	0.033	0	0.333	0.125
	t20	0.075	0	0	0.222	0	0	0.597	0.125	1	0.244	0.15	0.4	0.167	0	0.1	0.375
	t21	0	0.2	0.125	0	0.133	0.125	0.347	0.375	1	0.289	0.125	0.267	0.4	0	0.333	0.167
	t22	0.2	0.433	0.333	0	0	0	0.111	0.583	1	0.267	0.2	0.033	0.633	0	0.1	0.083
	t23	0.425	0.6	0.25	0	0	0	0	0.431	0.917	0.133	0.025	0.267	0.833	0.25	0	0.333
	t24	0.325	0.467	0.5	0	0	0	0.25	0.181	0.958	0.378	0.275	0.4	0.6	0	0.167	0.25

Appendix C: Case Study 2 Results

C.1 Generation Units

The percentage output of the generation units and the percentage power transferred for the initial and final cases are shown in Figure 22 and Figure 23 respectively.

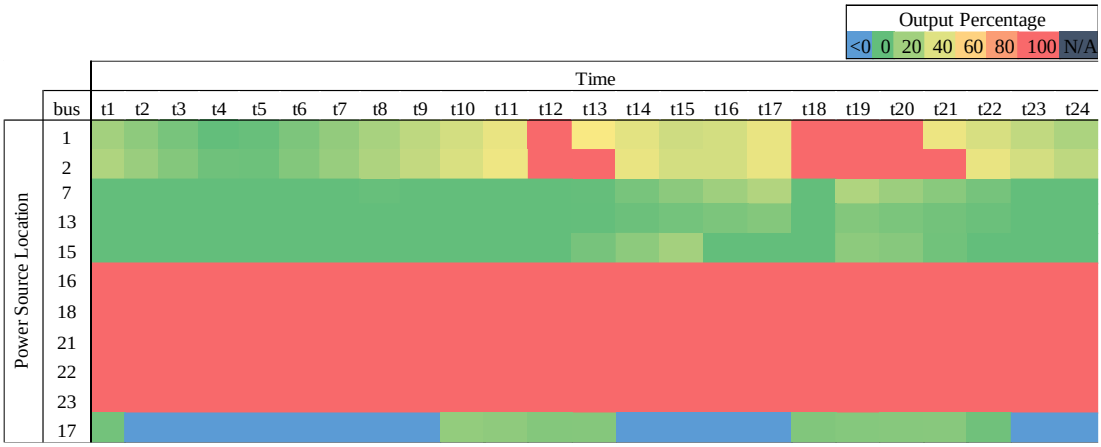

Figure 22 Percentage Output of The Generation Sources: Case Two-Initial Case

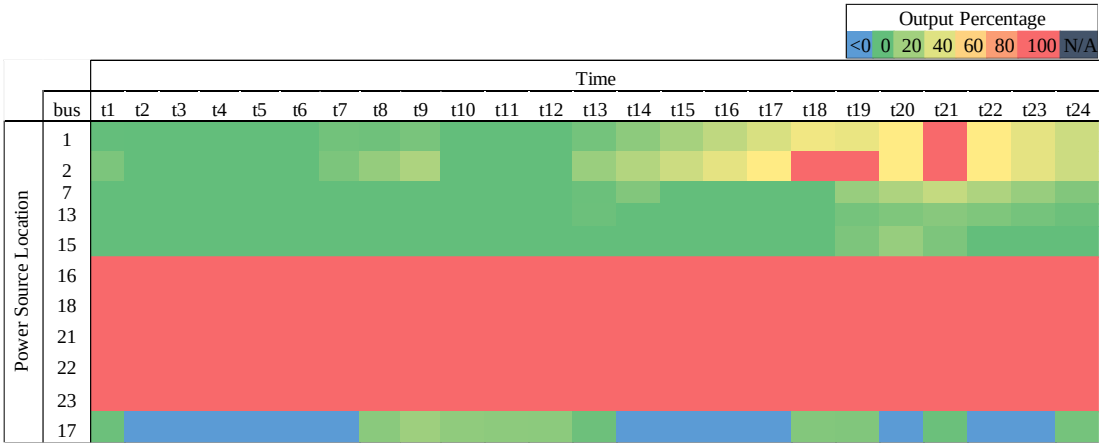

Figure 23 Percentage Output of The Generation Sources: Case Two-Final Case

The generation units on buses 16,18,21,22, and 23 are the cheapest to run, hence they are operating fully all day long in both cases. The units on buses 13 and 15 have the highest generation costs and therefore operate partially when needed. For example, in periods t18 → t20 in the initial case and in period t21 in the final case, when all the cheaper units are fully running units and the system requires more power, units on buses 13 and 15 operate, unlike previous periods.

In this case study, with the selling/purchasing prices being between the marginal costs of generating, the operator decides to sell power to the grid at several periods when the demand is not too high. On peak hours more power is needed and hence the operator decides to purchase electricity from the main grid to supply the loads in the most cost-effective way.

C.2 Industrial Load

Table 21 Machines Status: Case Two-Final Case

		Machine															
		r0.c1	r0.c2	r0.c3	r1.c1	r1.c2	r1.c3	r2.c1	r2.c2	r3.c1	r3.c2	r3.c3	r3.c4	r3.c5	r4.c1	r4.c2	r4.c3
Time	t1	0	0	0	0	0	0	0	0	0.21	0	0	0	0	0	0	0
	t2	0	0	0	0.01	0	0	0	0	0.46	0.02	0	0	0	0.23	0	0
	t3	0	0	0	0.26	0.03	0	0	0	0.71	0.16	0.08	0	0	0.48	0.23	0
	t4	0	0	0	0.36	0.17	0.13	0.13	0	0.96	0.33	0.03	0.03	0	0.63	0.47	0
	t5	0	0	0	0.61	0.33	0	0.38	0	1	0.09	0.23	0.2	0.23	0.88	0.23	0.25
	t6	0	0	0	0.86	0.1	0.08	0.25	0.24	1	0.24	0.1	0.27	0	1	0	0.33
	t7	0	0	0	1	0.03	0	0	0.01	1	0.47	0.3	0.43	0.17	1	0.2	0.25
	t8	0.15	0	0	0.97	0.2	0.25	0.24	0	0.96	0.31	0.18	0.23	0.23	1	0.43	0
	t9	0	0.13	0	0.88	0.27	0.25	0.49	0.08	1	0.29	0.15	0	0.47	1	0.23	0.04
	t10	0	0	0	0.7	0	0	0.7	0	1	0.3	0.1	0.2	0.2	1	0	0
	t11	0.05	0.13	0	0.44	0.27	0.04	0.92	0	1	0.29	0.05	0	0	0.75	0.03	0.25
	t12	0	0	0	0.19	0.3	0.25	1	0	0.88	0.22	0	0.23	0	0.5	0.27	0.5
	t13	0	0	0	0	0.17	0.04	0.86	0	0.83	0.13	0	0	0.23	0.25	0.5	0.75
	t14	0	0	0	0	0.4	0	0.64	0.25	1	0.36	0.18	0	0	0	0.73	1
	t15	0.15	0	0	0	0.63	0	0.89	0.5	0.96	0.16	0.43	0.23	0	0	0.9	1
	t16	0.3	0	0.1	0.1	0.4	0	0.6	0.3	1	0.4	0.2	0.5	0.2	0.2	0.7	1
	t17	0	0.2	0	0	0.2	0.3	0.4	0	1	0.2	0	0.4	0.5	0.1	0.5	0.8
	t18	0	0.27	0	0	0	0.04	0.24	0	0.83	0.24	0.18	0.23	0.37	0	0.23	0.5
	t19	0.23	0.03	0.08	0.01	0	0.08	0	0.14	1	0.27	0.25	0	0.23	0.15	0.23	0.25
	t20	0	0	0	0	0	0	0	0	0.92	0.02	0	0	0	0	0	0.08
	t21	0	0	0	0	0	0	0	0	0.75	0	0	0.03	0	0	0	0
	t22	0.03	0.23	0.17	0	0	0.17	0	0.15	0.92	0.18	0.03	0.2	0.23	0	0	0.13
	t23	0.25	0.47	0.42	0.22	0.23	0.42	0	0.4	1	0.42	0.23	0.43	0.47	0.1	0.2	0.38
	t24	0.5	0.7	0.58	0.47	0.47	0.67	0.19	0.64	1	0.67	0.48	0.67	0.7	0.35	0.33	0.54

Table 22 Number of Items in Buffers: Case Two-Final Case

		Buffer															
		r0.c1	r0.c2	r0.c3	r1.c1	r1.c2	r1.c3	r2.c1	r2.c2	r3.c1	r3.c2	r3.c3	r3.c4	r3.c5	r4.c1	r4.c2	r4.c3
Time	t1	0	0	0	0	0	0	0	0	5	0	0	0	0	0	0	0
	t2	0	0	0	1	0	0	0	0	14	1	0	0	0	9	0	0
	t3	0	0	0	16	1	0	0	0	17	2	3	0	0	14	7	0
	t4	0	0	0	22	0	3	9	0	10	15	3	1	0	11	21	0
	t5	0	0	0	26	10	3	36	0	26	1	6	0	7	32	22	6
	t6	0	0	0	76	9	5	3	17	28	4	2	8	7	72	14	14
	t7	0	0	0	144	10	5	0	18	10	1	1	16	12	100	14	20
	t8	6	0	0	190	4	5	17	0	5	1	1	16	7	114	27	2
	t9	2	4	0	221	0	11	34	6	3	2	7	2	21	140	33	3
	t10	2	4	0	265	1	11	86	6	3	4	6	1	28	180	33	3
	t11	0	8	0	265	7	10	152	0	1	13	8	1	24	208	28	3
	t12	0	8	0	243	4	16	224	0	2	23	1	8	24	212	24	15
	t13	0	8	0	223	7	17	286	0	10	29	1	1	31	192	21	33
	t14	0	8	0	175	19	17	278	18	2	31	8	1	31	148	19	57
	t15	6	8	0	99	38	11	234	36	11	4	18	8	19	94	22	63
	t16	16	4	2	56	51	1	226	24	3	2	13	15	6	60	19	57
	t17	11	9	2	33	45	7	257	24	8	11	1	13	20	36	15	75
	t18	3	17	2	33	43	8	274	24	6	8	1	9	31	22	10	87
	t19	11	14	4	34	39	1	244	7	6	0	11	2	20	14	11	66
	t20	11	14	4	34	39	1	244	7	26	1	11	2	20	14	9	68
	t21	11	14	4	34	39	1	244	7	44	1	10	3	20	14	9	68
	t22	5	13	8	34	31	4	211	15	50	7	5	2	25	14	6	68
	t23	1	7	18	22	18	4	124	14	36	8	1	1	19	6	3	47
	t24	0	0	32	0	0	0	0	0	0	0	0	0	0	0	0	0

The status of the machines in the final iteration are shown in Table 21. The number of items in the buffer is shown in Table 22. As in case study one, the machines abide by the work order and no machine operates unless the previous machine has produced enough items for it to function.

The non-binary nature of the machines' operation makes the industrial consumers better optimize their manufacturing lines as evidenced by the empty buffers in the machines at period t24, except the final buffer that accumulates all the final products. This shows that all resources are used efficiently, with a maximum number of outputs possible to make products to sell and a minimum purchase of items to start the manufacturing. Additionally, the ramping limits of the non-discrete operations are shown where the maximum difference is 0.25.

Appendix D: IEEE 123 Bus System

D.1 Network's Data

The updated IEEE 123 bus system in Figure 14 has 6 fuel-based generators. Their generation capacities, generation cost, and ramping limits are shown in Table 23. The base voltage is 4.16 kV with bus 1 being the slack bus.

Table 23 Fuel Based Generators Data: Case Three

DG number	1	2	3	4	5	6
Bus number	3	36	39	63	83	103
Pmax (kW)	1500	450	800	550	600	600
Pmin (kW)	0	0	0	0	0	0
Qmax (kvar)	726	250	387	265	289	289
Qmin (kvar)	0	0	0	0	0	0
Dr (kW)	750	112.5	320	165	180	180
Ur (kW)	750	112.5	320	165	180	180
a (¢/kW^2)	0.08	0.01	0.06	0.02	0.03	0.03
b (¢/kW)	0.70	0.08	0.45	0.20	0.23	0.20

Two wind turbines are connected at buses 71 and 113 and two PV systems are connected at buses 51 and 77. Their generation outputs throughout the day are listed in Table 24.

Table 24 Time-Varying Parameters: Case Three

Time	Wind - Bus 71 (kW)	Wind - Bus 113 (kW)	PV- Bus 51 (kW)	PV- Bus 77 (kW)	Ω	ϵt
t1	31.6	23.7	0	0	0.685	0.07
t2	34.8	26.1	0	0	0.644	0.07
t3	46.8	35.1	0	0	0.613	0.06
t4	103.6	77.7	0	0	0.6	0.05
t5	144.4	108.3	0	0	0.589	0.05
t6	226.8	170.1	0	0	0.598	0.06
t7	260.4	195.3	0	0	0.627	0.07
t8	226.8	170.1	106.6	80	0.652	0.08
t9	193.6	145.2	140.8	106	0.706	0.09
t10	219.2	164.4	181.4	136	0.787	0.12
t11	302.8	227.1	199.6	150	0.839	0.13
t12	284.4	213.3	200	150	0.853	0.14
t13	348.4	261.3	197	148	0.871	0.15
t14	372.8	279.6	194.6	146	0.834	0.16
t15	386.8	290.1	180.8	136	0.817	0.17
t16	400	300	157.8	118	0.819	0.18
t17	347.6	260.7	135.6	102	0.874	0.19
t18	266	199.5	102.2	76.7	1	0.18
t19	262.4	196.8	0	0	0.984	0.15
t20	224.4	168.3	0	0	0.936	0.13
t21	226	169.5	0	0	0.888	0.11
t22	222.4	166.8	0	0	0.809	0.09
t23	289.6	217.2	0	0	0.746	0.08
t24	336	252	0	0	0.733	0.07

Table 25 Line Data: Case Three

From	To	r(Ω)	x(Ω)	From	To	r(Ω)	x(Ω)	From	To	r(Ω)	x(Ω)	From	To	r(Ω)	x(Ω)
1	2	0.1605	1.6052	29	32	0.0566	0.0575	63	64	0.1258	0.1262	94	95	0.0692	0.0701
2	3	0.0350	0.0807	30	31	0.1258	0.1276	63	65	0.0175	0.0403	94	84	0.0175	0.0403
3	4	0.0441	0.0441	32	33	0.0755	0.0765	65	66	0.0504	0.0511	95	96	0.0881	0.0893
3	5	0.0628	0.0639	34	35	0.0261	0.0606	65	68	0.0218	0.0504	96	97	0.1006	0.1021
3	9	0.0261	0.0606	35	36	0.0306	0.0706	66	67	0.0755	0.0765	98	99	0.0504	0.0511
5	8	0.0504	0.0511	37	38	0.0350	0.0807	68	69	0.0132	0.0303	98	94	0.0241	0.0554
5	6	0.0817	0.0829	38	39	0.0175	0.0403	68	70	0.0218	0.0504	98	98	0.0218	0.0504
6	7	0.0628	0.0639	39	40	0.0109	0.0253	70	71	0.0218	0.0504	98	119	0.0241	0.0554
9	10	0.0175	0.0403	40	41	0.0241	0.0554	71	72	0.0218	0.0504	99	100	0.0692	0.0701
10	11	0.0566	0.0568	40	43	0.0306	0.0706	72	73	0.0436	0.1009	100	101	0.0817	0.0829
10	12	0.0566	0.0575	41	42	0.0241	0.0554	74	76	0.0692	0.0701	101	102	0.0692	0.0701
10	16	0.0261	0.0606	43	44	0.0630	0.0630	74	75	0.0261	0.0606	103	104	0.1132	0.1148
12	13	0.1070	0.1085	43	46	0.0656	0.1513	75	76	0.0504	0.0504	104	105	0.0755	0.0765
13	15	0.0628	0.0639	44	45	0.0630	0.0630	77	78	0.0755	0.0765	105	106	0.1447	0.1468
13	14	0.0628	0.0639	46	47	0.0481	0.1110	77	74	0.0197	0.0454	105	107	0.0315	0.0319
16	17	0.0377	0.0383	46	49	0.0720	0.0357	79	80	0.0566	0.0568	107	108	0.1321	0.1340
16	21	0.0722	0.1663	46	54	0.0054	0.1224	79	77	0.0197	0.0454	108	109	0.0817	0.0829
17	18	0.0251	0.0254	49	50	0.0504	0.0249	81	82	0.0440	0.0447	110	111	0.0566	0.0568
18	19	0.0943	0.0957	50	51	0.1007	0.0499	81	79	0.0241	0.0554	110	103	0.0284	0.0656
18	20	0.0881	0.0893	51	52	0.1224	0.0606	83	81	0.0393	0.0907	111	112	0.1447	0.1451
21	22	0.0628	0.0639	52	53	0.0936	0.0462	84	85	0.0350	0.0807	113	114	0.0566	0.0575
21	24	0.0261	0.0606	54	98	0.0306	0.0706	84	83	0.0611	0.1412	113	110	0.0241	0.0554
22	23	0.0817	0.0829	55	56	0.0327	0.0756	85	86	0.0087	0.0203	114	115	0.0817	0.0829
24	25	0.1322	0.1324	56	57	0.0568	0.1310	86	87	0.0197	0.0454	115	116	0.1760	0.1786
24	26	0.0218	0.0504	56	61	0.0218	0.0504	86	88	0.0415	0.0957	117	113	0.0218	0.0504
26	27	0.1383	0.1404	57	58	0.0755	0.0765	88	89	0.0415	0.0957	119	120	0.0481	0.1110
26	28	0.0241	0.0554	57	59	0.0630	0.0630	89	92	0.0218	0.0504	120	121	0.0261	0.0606
28	29	0.0306	0.0706	59	60	0.0819	0.0820	89	90	0.1698	0.1722	121	122	0.0699	0.1613
28	34	0.0175	0.0403	61	62	0.0817	0.0829	90	91	0.1194	0.1212	122	123	0.1605	1.6052
29	30	0.0241	0.0554	61	63	0.0218	0.0504	92	93	0.0218	0.0504				

The resistance (r) and the reactance (x) of the power lines are shown in Table 25. The sell/purchase price of transferred electricity is τ=¢18/kWh, with transferring limits of $P_{r,min}$=-300kW and$P_{r,max}$= +300kW on both transfer buses.

D.2 Residential Load Data

The residential loads at peak on each bus are shown in Table 26. To demonstrate the load throughout the day this load is multiplied by factor Ω shown in Table 24. The shifting limits ϵt are shown in Table 24 as well. 5% of the load is sheddable (y=5) and 80% is non-sheddable (z = 80).

Table 26 Peak Consumption on Buses: Case Three

Bus number	Pinitial (kW)	Qinitial (kW)	Bus number	Pinitial (kW)	Qinitial (kW)	Bus number	Pinitial (kW)	Qinitial (kW)
3	40	20	46	20	10	84	245	180
4	20	10	49	40	20	85	40	20
6	20	10	50	40	20	87	40	20
7	40	20	51	75	35	88	40	20
8	40	20	52	140	100	90	20	10
9	20	10	53	75	35	91	40	20
11	20	10	56	40	20	92	40	20
12	40	20	58	40	20	93	20	10
14	20	10	59	20	10	95	40	20
15	40	20	60	20	10	96	40	20
17	40	20	62	20	10	97	40	20
19	40	20	63	20	10	99	20	10
20	20	10	64	40	20	100	40	20
22	40	20	66	20	10	101	20	10
23	40	20	67	20	10	102	40	20
25	40	20	68	105	75	104	40	20
27	40	20	69	210	150	106	20	10
31	40	20	70	140	95	107	20	10
32	20	10	71	40	20	108	40	20
33	20	10	72	20	10	109	20	10
34	40	20	75	20	10	111	40	20
35	40	20	76	40	20	112	40	20
36	40	20	73	20	10	114	20	10
38	40	20	78	40	20	115	40	20
39	40	20	80	40	20	116	40	20
41	20	10	81	40	20	119	40	20
42	20	10	82	40	20	120	40	20
44	20	10	83	20	10	121	40	20
45	20	10						

D.3 Industrial Load Data

The scheme of the industrial load is shown in Figure 10 and its characteristics are shown in Table 27. The selling price of the final product is Ks =¢2500. The ramping

limit is ψ = 45%. The load is connected to bus number 5. The initial status of the machines for the day are shown in Table 28.

Table 27 Industrial Load Characteristics: Case Three

Machine	CT_{rc} (s)	CAP_{rc}	EOn_{rc}(kW)	α_{rc}	KP_r(¢)	β_r
r1.c1	50	300	60	4	1.2	6
r1.c2	120	100	40	2	0	0
r1.c3	150	100	24	1	0	0
r2.c1	50	300	30	3	1.5	4
r2.c2	50	300	40	3	0	0
r3.c1	150	300	20	2	2	3
r3.c2	80	100	20	2	0	0
r3.c3	90	100	30	1	0	0
r3.c4	120	100	20	1	0	0
r3.c5	120	100	20	2	0	0
r4.c1	90	300	10	2	1.2	3
r4.c2	120	100	20	1	0	0
r4.c3	150	100	30	3	0	0
r0.c1	90	500	50	1	2.4	2
r0.c2	120	500	40	2	0	0
r0.c3	150	2000	30	-	0	0

Table 28 Machines Status: Case Three-Initial Case

		Machine															
		r0.c1	r0.c2	r0.c3	r1.c1	r1.c2	r1.c3	r2.c1	r2.c2	r3.c1	r3.c2	r3.c3	r3.c4	r3.c5	r4.c1	r4.c2	r4.c3
Time	t1	0	0	0	0	0	0	0	0	0.417	0	0	0	0	0.025	0	0
	t2	0	0	0	0	0	0	0.139	0	0.833	0	0	0	0	0.475	0.033	0
	t3	0	0	0	0.444	0	0	0.583	0.014	1	0.067	0	0	0	0.925	0.467	0.333
	t4	0	0	0	0.889	0.433	0	1	0	1	0	0.025	0	0	1	0.9	0.75
	t5	0	0	0	1	0	0	1	0	1	0.244	0.15	0.067	0	1	0.467	0.792
	t6	0	0	0	1	0.433	0.042	1	0	1	0.022	0	0	0.033	1	0.467	1
	t7	0.025	0	0	0.556	0.567	0.458	0.556	0.292	1	0.467	0.175	0.367	0.333	0.975	0.567	0.583
	t8	0.3	0.1	0	1	1	0.875	1	0.736	1	0.911	0.6	0.8	0.767	1	1	1
	t9	0.25	0.533	0.375	1	1	0.75	1	0.889	1	0.467	0.25	0.367	0.433	1	1	1
	t10	0.025	0.167	0	0.861	0.567	0.375	0.889	0.444	1	0.178	0.125	0	0.033	1	0.6	0.917
	t11	0	0	0	0.431	0.133	0	0.444	0	1	0.378	0	0	0	0.7	0.433	0.5
	t12	0	0	0	0	0	0	0	0	1	0	0	0.1	0	0.25	0	0.083
	t13	0	0	0	0	0	0	0	0	0.875	0.022	0	0	0.033	0	0	0
	t14	0.05	0	0	0	0.167	0	0.444	0.014	1	0.422	0.45	0.367	0.333	0.45	0.433	0.375
	t15	0.3	0.333	0.292	0.375	0.233	0.292	0.444	0.444	1	0.578	0.325	0.633	0.667	0.4	0.433	0.792
	t16	0.125	0.233	0.125	0	0	0	0	0	0.708	0.133	0.075	0.2	0.233	0	0	0.375
	t17	0	0	0	0	0	0.042	0	0	1	0.333	0.2	0	0	0	0	0
	t18	0	0	0	0	0	0	0	0	1	0	0	0.167	0.167	0	0	0
	t19	0	0	0	0	0	0	0	0	0.833	0.022	0	0	0	0	0	0
	t20	0	0	0	0	0	0	0	0	1	0	0	0	0	0	0	0
	t21	0	0	0	0	0	0	0	0	1	0.156	0.1	0	0	0	0	0
	t22	0	0	0	0	0	0	0	0	1	0.111	0	0.167	0.133	0	0	0
	t23	0.15	0.233	0.125	0	0	0	0	0	1	0.556	0.325	0.467	0.467	0	0	0
	t24	0.475	0.667	0.5	0	0	0	0	0	1	0.978	0.6	0.833	0.9	0	0	0

Appendix E: Case Study 3 Results

E.1 Generation Units

The percentage output of the generation units and the percentage power transferred for the initial and final cases are shown in Figure 24 and Figure 25 respectively.

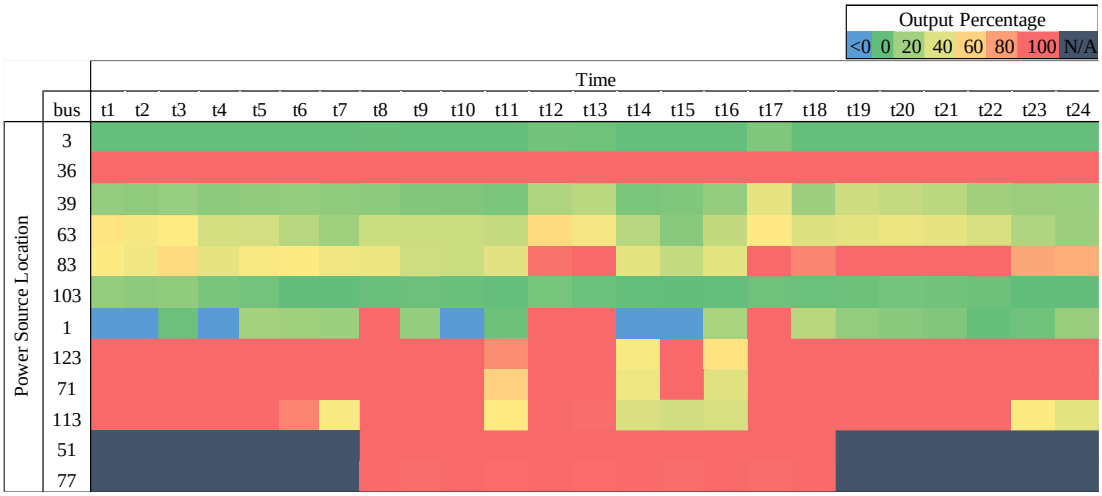

Figure 24 Percentage Output of The Generation Sources: Case Three-Initial Case

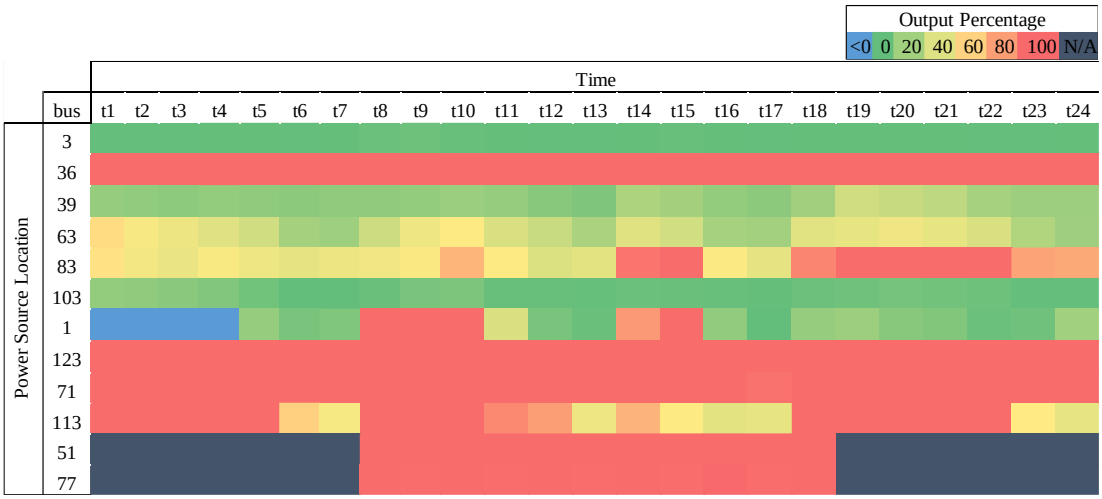

Figure 25 Percentage Output of The Generation Sources: Case Three-Final Case

The PV and wind turbine units on buses 71,113,51, and 77 operate almost fully throughout the day due to their zero generation costs. Interestingly, the wind turbines on buses 71 and 113 do not always operate at full capacity due to the physical constraints of the network. The units on buses 3 and 103 have the highest generation costs and therefore operate partially when needed. The other units in addition to the transferred power bus have power costs between the previously mentioned power sources and therefore their generation output varies the most throughout the day.

E.2 Industrial Load

The status of the machines in the final iteration is are shown in Table 29. The number of items in the buffer is shown in Table 30. Again, the outputs verify the optimal behavior of industrial load in the elastic mode of operations. The buffers at the last period are empty except the last buffer that contains the whole outputs. The 45% ramping limits are abided in addition to the order of operation and items generation.

Table 29 Machines Status: Case Three-Final Case

		Machine															
		r0.c1	r0.c2	r0.c3	r1.c1	r1.c2	r1.c3	r2.c1	r2.c2	r3.c1	r3.c2	r3.c3	r3.c4	r3.c5	r4.c1	r4.c2	r4.c3
Time	t1	0	0	0	0	0	0	0	0	0.417	0	0	0	0	0.025	0	0
	t2	0	0	0	0.014	0	0	0.083	0	0.833	0.044	0	0	0	0.45	0.033	0
	t3	0	0	0	0.444	0.033	0	0.528	0	1	0.111	0.075	0	0	0.9	0.367	0.333
	t4	0	0	0	0.556	0	0	0.556	0	1	0	0	0.033	0	0.925	0.367	0.583
	t5	0	0	0	1	0.433	0.083	1	0.069	1	0.444	0.075	0.1	0.1	1	0.8	1
	t6	0.025	0	0	1	0.3	0	1	0	1	0	0.05	0	0	1	1	1
	t7	0.025	0.033	0	0.681	0.433	0.292	1	0.292	1	0.378	0.175	0.333	0.333	1	0.567	0.958
	t8	0.4	0.433	0.25	0.889	0.867	0.708	0.889	0.736	1	0.822	0.625	0.767	0.767	0.9	0.867	0.833
	t9	0	0	0	0.444	0.433	0.292	0.444	0.292	1	0.378	0.225	0.367	0.333	0.45	0.433	0.417
	t10	0	0	0	0	0	0	0	0	0.917	0.133	0	0	0	0	0	0
	t11	0	0	0	0	0	0	0.153	0	1	0.022	0.025	0	0	0.375	0	0.25
	t12	0.25	0.4	0.208	0.444	0.433	0.417	0.597	0.444	1	0.467	0.275	0.4	0.433	0.825	0.433	0.667
	t13	0.175	0.267	0	0.444	0.433	0.292	0.444	0.389	1	0.444	0.3	0.4	0.4	0.45	0.433	0.417
	t14	0	0	0	0	0	0	0	0	1	0	0	0	0	0	0	0
	t15	0	0	0	0	0	0	0	0	1	0.111	0	0	0	0	0	0
	t16	0	0	0	0.444	0.267	0.125	0.444	0	1	0.356	0.25	0.333	0.333	0.45	0.333	0.417
	t17	0.3	0.367	0.375	0.708	0.6	0.417	0.778	0.417	1	0.578	0.325	0.433	0.433	0.8	0.7	0.833
	t18	0	0	0.042	0.264	0.167	0	0.333	0	1	0.133	0.05	0.067	0.033	0.35	0.267	0.417
	t19	0	0	0	0	0	0	0	0	0.583	0	0	0	0.033	0	0	0
	t20	0	0	0	0	0	0	0	0	0.75	0	0	0	0	0	0	0
	t21	0	0	0	0	0	0	0	0	1	0	0	0	0	0	0	0
	t22	0	0	0	0	0	0	0	0	1	0.067	0	0	0	0	0	0
	t23	0.125	0.167	0.083	0	0	0	0	0	0.958	0.511	0.35	0.433	0.4	0	0	0
	t24	0.35	0.533	0.417	0	0	0.125	0	0.111	0.542	0.867	0.5	0.733	0.8	0	0	0.125

Table 30 Number of Items in Buffers: Case Two-Final Case

		Buffer															
		r0.c1	r0.c2	r0.c3	r1.c1	r1.c2	r1.c3	r2.c1	r2.c2	r3.c1	r3.c2	r3.c3	r3.c4	r3.c5	r4.c1	r4.c2	r4.c3
Time	t1	0	0	0	0	0	0	0	0	10	0	0	0	0	1	0	0
	t2	0	0	0	1	0	0	6	0	26	2	0	0	0	17	1	0
	t3	0	0	0	29	1	0	44	0	40	1	3	0	0	31	4	8
	t4	0	0	0	69	1	0	84	0	64	1	2	1	0	46	1	22
	t5	0	0	0	89	10	2	141	5	48	15	2	1	3	38	1	46
	t6	1	0	0	125	19	1	213	2	72	11	4	1	1	18	7	67
	t7	1	1	0	122	18	7	222	20	62	14	1	1	9	24	1	87
	t8	4	2	6	82	10	8	127	25	12	1	3	1	0	8	7	59
	t9	4	2	6	62	9	15	96	46	2	0	1	2	10	0	10	69
	t10	4	2	6	62	9	15	96	46	12	6	1	2	10	0	10	69
	t11	4	2	6	62	9	15	107	46	34	5	2	2	10	15	4	75
	t12	2	4	11	42	2	15	54	48	16	4	1	1	3	22	1	61
	t13	1	12	11	22	1	15	2	55	0	0	1	1	1	14	4	50
	t14	1	12	11	22	1	15	2	55	24	0	1	1	1	14	4	50
	t15	1	12	11	22	1	15	2	55	38	5	1	1	1	14	4	50
	t16	1	12	11	22	3	18	34	55	30	1	1	1	11	12	4	60
	t17	2	5	20	1	1	16	0	49	2	1	1	1	0	2	5	44
	t18	2	3	21	0	6	16	24	49	14	3	1	2	1	0	3	54
	t19	2	3	21	0	6	16	24	49	28	3	1	1	2	0	3	54
	t20	2	3	21	0	6	16	24	49	46	3	1	1	2	0	3	54
	t21	2	3	21	0	6	16	24	49	70	3	1	1	2	0	3	54
	t22	2	3	21	0	6	16	24	49	88	6	1	1	2	0	3	54
	t23	2	4	23	0	6	11	24	34	65	1	2	2	4	0	3	39
	t24	0	0	33	0	0	0	0	0	0	0	0	0	0	0	0	0

End of document